universität wien

MASTERARBEIT | MASTER'S THESIS

Titel | Title

Influence of PCNA on the expression of genes encoded by the ϕCh1 virus infecting the archaeon N. magadii

verfasst von | submitted by

Ermirë Jerliu

angestrebter akademischer Grad | in partial fulfilment of the requirements for the degree of

Master of Science (MSc)

Wien | Vienna, 2024

Studienkennzahl lt. Studienblatt | Degree programme code as it appears on the student record sheet:	UA 066 830
Studienrichtung lt. Studienblatt | Degree programme as it appears on the student record sheet:	Masterstudium Molecular Microbiology, Microbial Ecology and Immunobiology
Betreut von | Supervisor:	ao. Univ.-Prof. Dipl.-Biol. Dr. Angela Witte

Acknowledgments

First and foremost, I would like to express my deepest gratitude to my supervisor Ao. Univ.-Prof. Dipl.-Biol. Dr. Angela Witte for her invaluable guidance, support, and patience throughout this entire journey. The time spent in her lab was a truly formative experience, and I will forever cherish the wisdom, laughter, and encouragement she so generously shared. Angela is not only an exceptional scientist but also a wonderful person, and I feel incredibly fortunate to have had her as my mentor.

I would also like to extend my sincere thanks to my incredible colleagues, Clara, Benni, Helene, Roland, and Hena, for all their support throughout this journey. Your assistance in the lab was invaluable, but it was the shared jokes and fun times that truly made this experience unforgettable. I deeply appreciate Alex for his assistance in reviewing this work and for always being ready to help.

I owe my deepest gratitude to my parents and my brother for being my biggest supporters throughout my studies. You have been behind me every step of the way, sacrificing so much to help me achieve this goal. Your unwavering belief in me and constant encouragement have been the foundation of my success, and I truly couldn't have done this without you. Thank you for everything.

Abstract

The ORF59 of ϕCh1 virus, infecting the halophilic archaeon *N. magadii*, encodes a putative proliferating cell nuclear antigen (PCNA) with high sequence similarity to the host-encoded PCNA, suggesting recent horizontal gene transfer. PCNA, a processivity factor in DNA replication, is rare in dsDNA viruses, especially in Archaea. Previous research showed that viral PCNA is crucial for ϕCh1 replication, with its deletion severely impacting viral progeny, protein synthesis, and cell lysis. However, its specific effect on key viral and host proteins, remained unstudied in a virus-cured strain, making ϕCh1 PCNA a unique target for study.

This study aimed to determine whether PCNA directly or indirectly affects the expression of methyltransferase and gp34 proteins encoded by ϕCh1 in *N. magadii* strain L13. Three PCNA variants, namely wild-type, mutated (GTG → ATG) and a truncated version with ATG as start codon were cloned into *N. magadii* L13 and analysed both in cis, where PCNA and the target gene (gp34) were on the same plasmid, and trans with PCNA and ORF94 (methyltransferase) located on separate plasmids. Based on growth kinetics and Western blot analyses, the different PCNA variants demonstrate distinct effects on methyltransferase and gp34 production. Although PCNA plays a direct role in enhancing the expression of both proteins, it is not strictly essential for their synthesis. In addition to the wild-type ORF94, a construct containing a mutated upstream region of ORF94 was designed to investigate whether alterations in the upstream regulatory region affect the binding and subsequent expression of the methyltransferase. The results suggest that this mutation does indeed impact methyltransferase expression, indicating that changes in the upstream regulatory region interfere with proper regulation and binding, ultimately affecting protein production.

KEYWORDS: φCh1, Archaea*, N. magadii*, cured strain L13, PCNA, Methyltransferase, tail-fibre gp34

Zusammenfassung

Das ORF59 des ϕCh1-Virus, das das halophile Archaeon *N. magadii* infiziert, kodiert ein putatives proliferierendes Zellkernantigen (PCNA), das eine hohe Sequenzähnlichkeit zum vom Wirt kodierten PCNA aufweist, was auf einen kürzlichen horizontalen Gentransfer hindeutet. PCNA, ein Prozessivitätsfaktor in der DNA-Replikation, ist selten in dsDNA-Viren, insbesondere in Archaea, was das ϕCh1-PCNA zu einem einzigartigen Untersuchungsziel macht.

Frühere Forschungen zeigten, dass virales PCNA für die ϕCh1-Replikation entscheidend ist, wobei seine Deletion die Virusnachkommen, die Proteinsynthese und die Zelllyse stark beeinträchtigt. Seine spezifische Wirkung auf wichtige virale und Wirtsproteine blieb jedoch in einem virusbefreiten Stamm unerforscht.

Diese Studie zielte darauf ab zu bestimmen, ob PCNA die Expression von Methyltransferase und gp34-Proteinen, die von ϕCh1 in *N. magadii*-Stamm L13 kodiert werden, direkt oder indirekt beeinflusst. Drei PCNA-Varianten, darunter: (1) Wildtyp-PCNA des Virus mit dem GTG-Codon, (2) eine Variante, bei der das GTG-Codon in ATG geändert wurde, und (3) eine verkürzte Version, die mit ATG beginnt und der Größe des vom Wirt kodierten PCNA entspricht, wurden in *N. magadii* L13 kloniert und in zwei Systemen analysiert: in cis, wo PCNA und das Zielgen (gp34) auf demselben Plasmid waren, und in trans, wo PCNA und ORF94 (Methyltransferase) auf separaten Plasmiden waren. Basierend auf Wachstumskinetik- und Western-Blot-Analysen zeigen die verschiedenen PCNA-Varianten unterschiedliche Auswirkungen auf die Produktion von Methyltransferase und gp34. Obwohl

PCNA eine direkte Rolle bei der Steigerung der Expression beider Proteine spielt, ist es für ihre Synthese nicht unbedingt erforderlich. Neben dem Wildtyp-ORF94 wurde eine zweite Konstruktion, die eine mutierte regulatorische Region stromaufwärts von ORF94 (ORF94-M-M1_2) enthält, entwickelt, um zu untersuchen, ob Veränderungen in der regulatorischen Region die Bindung und die nachfolgende Expression der Methyltransferase beeinflussen. Die Ergebnisse zeigten, dass diese Mutation die Expression der Methyltransferase tatsächlich beeinflusst, was darauf hindeutet, dass Änderungen in der regulatorischen Region die ordnungsgemäße Regulation und Bindung stören und letztlich die Proteinproduktion beeinträchtigen.

SCHLÜSSELWÖRTER: φCh1, *Archaea, N. magadii*, ausgehärter Stamm L13, PCNA, Methyltransferase, gp34

Table of Contents

1. Introduction

1.1. Archaea

Archaea are prokaryotic organisms forming the third domain of life. They were initially classified as bacteria but phylogenetic analysis of 16S rRNA sequences revealed that they are evolutionarily distinct (Woese and Fox, 1977) . Initially discovered in extreme environments, such as hot springs and hydrothermal vents, archaea have since been found in a wide range of habitats, including highly saline, acidic, and anaerobic environments (Pikuta *et al.*, 2007; Valentine, 2007). Culture-independent methods further demonstrated their presence in mesophilic terrestrial and marine ecosystems (DeLong, 1992), highlighting their adaptability and ecological significance. Recent studies indicate a strong connection between eukaryotes and Asgard Archaea, with Heimdallarchaeota emerging as the most likely closest archaeal relatives to the eukaryotic nuclear lineage (Williams *et al.*, 2019), highlighting the intriguing nature of archaea and their evolutionary significance.

Currently, three main phyla are recognized within the domain of Archaea, based on the RNA component of the small ribosomal subunit: the Euryarchaeota (containing mostly methanogens, halophiles, and hyperthermophiles), the Crenarchaeota (consisting mostly of sulfur-dependent thermophiles) (Woese, 1990) and the Thaumarchaeota (mostly mesophilic) (Brochier-Armanet *et al.*, 2008). Over the years, studies on the Archaea have revealed that these organisms are rather peculiar: although they resemble bacteria in their cellular and genomic organization, their transcriptional and translational machinery is more similar to that seen in the Eukaryotes (Olsen and Woese, 1977; Bernander, 2000).

The most notable feature of archaea is the absence of a peptidoglycan cell wall (Howland, 2000) and the unique composition of their cell membranes. Except for some methanogenic archaea that have a peptidoglycan variant called pseudopeptidoglycan (Willmer, 2000; Woese, 1978), their cell walls do not contain the typical peptidoglycan. Instead, a common

cell wall structure in the archaeal domain is a paracrystalline protein surface layer, known as the S-layer, composed of one or two types of glycoproteins (Rodrigues-Oliveira *et al.*, 2017; Sleytr & Beveridge, 1999) . Archaeal glycoproteins were also the first proteins in prokaryotes found to be glycosylated (Mescher and Strominger, 1976). The archaeal cell membranes consist of various isoprenoid chains stereospecifically ether-linked to sn-glycerol 1-phosphate head groups. In contrast, eukaryotic and bacterial membranes are composed of fatty acids ester-linked to sn-glycerol 3-phosphate (Albers and Meyer, 2011). Ether bonds in archaeal membranes are significantly more resistant to hydrolysis than ester bonds when exposed to extreme conditions such as high osmotic pressure, extreme pH and high temperatures (Tenchov *et al.*, 2006; Van De Vossenberg, J. L. C. M. *et al.*, 1999).

1.1.1. Halophilic archaea

Hypersaline environments, which are widely distributed on Earth and found in aquatic systems like salt lakes and saline soils, commonly host halophilic archaea, such as Haloarchaea that thrive in water-saturated areas with high evaporation rates leading to hypersalinity (De La Haba *et al.*, 2011; Oren, 2002). Microorganisms that inhabit these saline environments are known as halophiles.

These microorganisms need high salt concentrations for growth and survival. They are classified into two subcategories based on their salt requirements: moderate halophiles, which grow optimally at 0.5 to 2.5 M NaCl, and extreme halophiles, which thrive at environments with elevated salt concentrations (2.5 to 5 M NaCl) (Andrei, Banciu and Oren, 2012).

Halophilic archaea, which are aerobic or facultatively anaerobic and red-pigmented, belong to the archaeal domain (Wais *et al.*, 1975; Grant *et al.*, 2001). Their aquatic habitats often appear pink-red due to the presence of carotenoid pigments produced by these organisms (Oren, 2014). Most haloarchaea are part of the family *Halobacteriaceae* (phylum

Euryarchaeota) and include around 50 genera of extreme halophiles (Oren, 2014). However, some haloarchaea are also classified as methanogens (Andrei *et al.*, 2012).

Haloarchaea have evolved a specialized strategy to cope with the high osmotic pressure in hypersaline environments, known as the "salt-in" mechanism. To manage the extreme salt concentrations, these microorganisms utilize Na+/H+ antiporter membrane proteins to expel sodium ions from the cell while accumulating potassium chloride within the cytoplasm (Fendrihan *et al.*, 2006; Oren, 1999). In these extremophiles, intracellular potassium levels can reach up to 5 M (Christian and Waltho, 1962; Lai and Gunsalus, 1992). Despite the risk of protein precipitation at such high potassium chloride concentrations, halophilic enzymes are adapted with a high proportion of negatively charged acidic amino acids and a low isoelectric point, which helps maintain their stability (Oren, 1999). Haloarchaea not only tolerate but actually require molar salt concentrations for their cellular functions and growth. They have undergone significant structural and biochemical adaptations to endure high osmotic pressure. The 'salt-in' approach helps balance extracellular and intracellular salt concentrations by maintaining equimolar levels of salt inside the cell.

Another method to manage high osmotic pressure is through the accumulation of organic solutes, such as glycerol, either by synthesizing them *de novo*, a capability unique to methanogens (Lai *et al.*, 1991), or by absorbing them from the environment.

It has been observed that proteins of haloarchaea are largely adapted to contain high levels of acidic amino acids (glutamate and aspartate) and low levels of basic amino acids (lysine and arginine), as well as a reduced fraction of basic, hydrophobic residues, necessitating high salt concentrations to maintain protein-protein interactions (Bitan-Banin, Ortenberg and Mevarech, 2003; Lanyi ; Oren).

1.1.2. Haloalkaliphilic archaea

The term "haloalkaliphilic" was coined by Soliman and Trüper (1982) (Soliman and Trüper, 1982) to describe a newly isolated archaeon that was both halophilic and alkaliphilic. This term is now used for various archaea that require high salt concentrations and very alkaline pH (pH 8–11) for optimal growth (Sorokin *et al.*, 2019, 2018; Tindall *et al.*, 1984; Xue *et al.*, 2005). Haloalkaliphilic archaea thrive in hypersaline alkaline environments, such as Lake Magadi in Kenya, which has salt concentrations up to 300 g/L, high levels of carbonate ions, and a pH above 11 (Ma *et al.*, 2010; Oren 1999).

1.1.2.1. Natrialba magadii

Natrialba magadii is a haloalkaliphilic archaeon isolated from the alkaline soda lake Lake Magadi in Kenya (Tindall *et al.*, 1984). Initially classified within the genus *Natronobacterium* based on phenotypic properties and lipid composition, it was reclassified into the genus *Natrialba* within the family *Halobacteriaceae* of the phylum Euryarchaeota following phylogenetic analysis of the 16S rRNA (Kamekura *et al.*, 1997). *N. magadii* is a dual extremophile, requiring high salt concentrations (3.5 - 4 M NaCl) and high pH (9.5 - 11) for growth, with an optimal temperature range of 37 - 42 °C. It also requires low Mg^{2+} concentrations (below 10 mM). Metabolically, *N. magadii* is an obligate aerobe and proteolytic chemoorganotroph, utilizing amino acids and peptides as sole carbon sources and incapable of processing carbohydrates (Tindall *et al.*, 1984). The cells are rod-shaped, flagellated, and exhibit an orange/red colour due to carotenoids in their membranes. Notably, *N. magadii* is polyploid, containing multiple copies of its genome per cell, and has a generation time of approximately 9 hours (Breuert *et al.*, 2006).

Two different strains of *Natrialba magadii* are used for laboratory work: L11 and L13 (see Figure 1). *N. magadii* L11 is the wild type strain that contains the φCh1 virus, which causes

lysis of the host cell and provides immunity to superinfection. In contrast, *Nab. magadii* L13, derived by continuous passaging of the wild type, is cured of the provirus and is non-lysogenic, making it susceptible to φCh1 infection and useful as an indicator strain (Witte *et al.*, 1997). Notably, *N. magadii* is the only known host of φCh1.

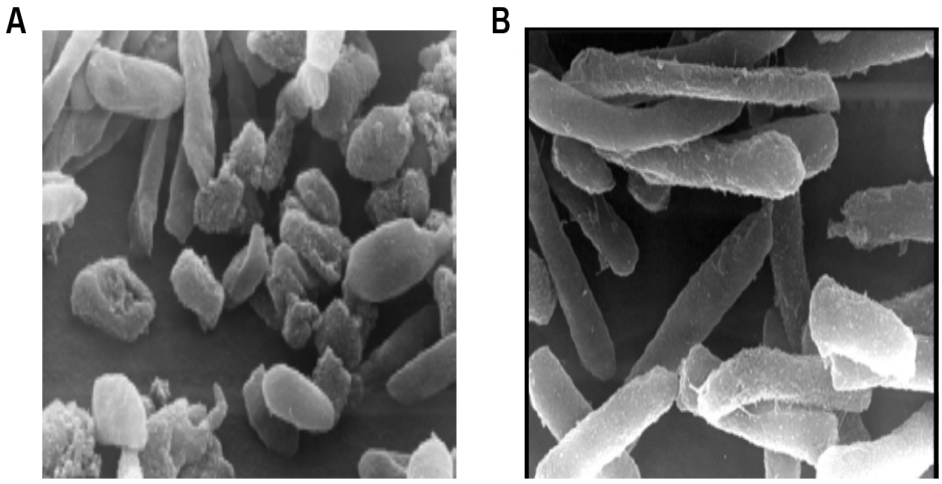

Figure 1. Electron micrographs of the haloalkaliphilic archaeon *Natrialba magadii*, initially isolated from Lake Magadi (Kenya). (A) Wild type strain L11 carrying φCh1 as a prophage. (B) Strain L13, cured from the virus *(Iro et al., 2007)*.

1.1.2.2. Genetic techniques for manipulating halophilic Archaea

Genetic engineering is crucial for understanding gene functions and is widely applied. However, genetic manipulations in *N. magadii* are challenging due to its polyploidy, long generation times and limited genetic tools, often necessitating the use of *E. coli* for such manipulations. In general, genetic studies in Archaea face difficulties compared to Bacteria and Eukarya due to the lack of selective markers and suitable plasmid systems. In addition, many archaea are inherently resistant to antibiotics commonly used in bacterial genetic systems.

1.1.2.2.1. Shuttle vectors and selection markers

Vectors are essential tools for studying halophilic archaeal genes and enzymes, though only a few are available. Currently, two shuttle vectors, pNB102 and pRo5, are used for *N. magadii* and both were used for the purpose of this study.

The pRo5 vector, which is based on the *E. coli* vector pKSII+, consists of a mutated DNA gyrase gene (*gyrB*), conferring novobiocin resistance, and the bla gene for ampicillin resistance in *E. coli*. It also contains the minimal replicon of φCh1 (ORF53 and ORF54) necessary for replication in *N. magadii*, which includes AT-rich regions homologous to the RepH protein, essential for replication in halophilic archaea (Mayrhofer-Iro *et al.*, 2013; Ng and DasSarma, 1993). The second vector, namely pNB102, is derived from the plasmid pNB101 from *Natronobacterium sp.* AS7091 by adding the ColE1 origin for autonomous replication in *E. coli* and resistance cassettes for ampicillin and mevinolin, the latter inhibiting archaeal lipid synthesis for selection in haloarchaea (Lam and Doolittle, 1992; Zhou *et al.*, 2004).

1.1.2.2.2. Transformation

The first transformation method in halophilic archaea was reported for *Halobacterium salinarum* using a PEG (polyethylene glycol 600) mediated transformation technique (Cline and Doolittle, 1987). Treatment with EDTA, which acts as a chelating agent, removes the S-layer and results in the generation of spheroplasts. This technique was later adapted for *Haloferax volcanii* (Charlebois *et al.*, 1987). However, this method proved inefficient for the extreme alkalophile *N. magadii* due to its sturdy S-layer, which differs significantly from that of moderate halophiles (Mengele and Sumper, 1992). To address this, the method was modified for *N. magadii* by incubating cells with bacitracin to destabilize the S-layer by impeding glycosylation of surface proteins, followed by proteinase K treatment to remove the

weakened S-layer. This process successfully led to the formation of spheroplasts that could be transformed via the PEG-mediated method (Mayrhofer-Iro *et al.*, 2013).

1.2. Viruses of archaea

Archaeal viruses exhibit a unique blend of physiological and morphological characteristics not found in viruses that infect the other two domains of life (Hartman *et al.*, 2019; Krupovic *et al.*, 2018). Discovered in *Halobacterium cutirubrum* and *Halobacterium salinarium*, the first archaeal virus described had a typical head-and-tail morphology, leading to its initial misidentification as a bacteriophage (Torsvik and Dundas, 1974). Since then, archaeal viruses have been isolated from halophilic hosts, methanogens, and thermophiles (Torsvik and Dundas, 1980; Janekovic *et al.*, 1983; Martin *et al.*, 1984; Wais *et al.*, 1975). To date, over 130 archaeal viruses have been identified across various environmental settings (Dellas *et al.*, 2014; Pietilä *et al.*, 2014). These viruses inhabit a variety of ecosystems, including extreme acidic, thermal, and saline environments where archaeal organisms flourish, with hosts ranging from halophilic microorganisms to thermophiles (Janekovic *et al.*, 1983; Martin *et al.*, 1984; Torsvik and Dundas, 1980).

Archaeal viruses are categorized into archaea-specific viruses and cosmopolitan archaeal viruses (Iranzo *et al.*, 2016). Archaea-specific viruses exhibit extensive diversity and unique morphological characteristics (Arnold *et al.*, 2000; Häring *et al.*, 2005; Krupovic *et al.*, 2014) and are divided into 12 families. Conversely, cosmopolitan archaeal viruses are dsDNA viruses classified within the order Caudovirales. They have an icosahedral head and long tails, either contractile (*Myoviridae*) or noncontractile (*Siphoviridae*) (Senčilo and Roine, 2014). Most identified viruses belong to the phyla Euryarchaeota and Crenarchaeota.

1.2.1. Haloarchaeal viruses

Halophilic archaea are host to the most abundant group of archaeal viruses, with around 90 of the approximately 130 known archaeal viruses infecting haloarchaea (Luk *et al.*, 2014; Pietilä *et al.*, 2013; Prangishvili, 2013; Tang *et al.*, 2002). The first two described archaeal viruses were halophilic, both from the *Halobacteriaceae* family (Torsvik and Dundas, 1974; Wais *et al.*, 1975). Most haloarchaeal viruses are tailed icosahedral viruses (Caudovirales) with dsDNA genomes, although some pleomorphic and spindle-shaped forms exist (Ackermann and Prangishvili, 2012; Luk *et al.*, 2014).

Haloarchaeal viruses belong to various families, such as *Myoviridae*, *Siphoviridae*, *Podoviridae*, *Pleioviridae*, *Pleolipoviridae*, *Sphaerolipoviridae*, and *Fuselloviridae*, each exhibiting distinct morphologies. Some resemble other viruses or bacteriophages, while others have unique lifecycle and morphological traits. Research on haloarchaeal viruses is relatively limited compared to bacteriophages and viruses infecting eukaryotes, partly due to the challenges in cultivating haloarchaea. However, studies have revealed significant novelty in certain haloarchaeal viruses (Luk *et al.*, 2014). Haloarchaeal viruses similar to their hosts, have proteins adapted to high salt concentrations. These proteins are generally acidic (below pH 6) resulting in a negative charge that promotes salt bridge formation, water molecule attraction, and the development of hydration shells around the proteins (Luk *et al.*, 2014).

Haloarchaeal viruses interact with their hosts in temperate, lytic, and chronic ways, with persistent infections being common (Luk *et al.*, 2014; Roine and Oksanen, 2011). Notable examples include the best studied viruses of *Halobacteriaceae* φH and φCh1. The temperate φH virus, which infects *Halobacterium salinarum* and exists as a plasmid in the cytoplasm without integrating into the host genome, and φCh1, which integrates into the *Natrialba magadii* chromosome (Klein *et al.*, 2002; Schnabel *et al.*, 1982; Witte *et al.*, 1997). Both

viruses share high sequence similarity despite their phylogenetically distant hosts (Klein *et al.*, 2002). Another example is HF1 and HF2, the first reported lytic haloarchaeal viruses, capable of infecting multiple hosts like *Haloferax* and *Halobacterium*, and showing more than 80% genome similarity(Dyall-Smith *et al.*, 2003). Other lytic viruses, such as Ja.1 and B10, have also been discovered but are less well understood (Porter *et al.*, 2007).

1.2.2. The haloalkalophilic virus φCh1

The φCh1 virus, which infects the haloalkaliphilic archaeon *Natrialba magadii*, is a temperate virus belonging to the *Myoviridae* family. It features a head-tail morphology, with a 70 nm icosahedral head and a 130 nm long contractile tail, resulting in a total length of approximately 200 nm (Figure 2). Its linear double-stranded DNA genome (58.5 kbp) is packed together with host-encoded RNA, the function of which remains unknown but might be related to DNA packaging. The virus integrates as a provirus in the chromosomal DNA of its host and can switch between lysogenic and lytic states, with spontaneous lysis occurring in the stationary phase, indicating growth-dependent lysis (Witte *et al.*, 1997). ΦCh1 can infect the cured *N. magadii* L13 strain but shows immunity to superinfection (Witte *et al.*, 1997). Due to the extreme conditions in which its host thrives, the virus has adapted to meet its host's physiological needs. ΦCh1 requires salt concentrations above 2 M to maintain its infectivity and stability; lower salt levels may lead to the dissociation of virus particles or conformational changes in the capsid proteins (Witte *et al.*, 1997).

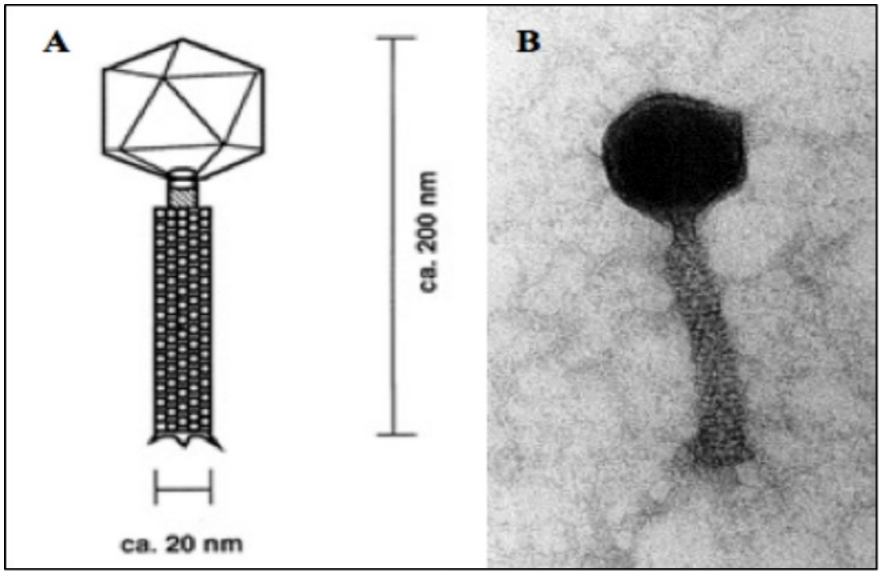

Figure 2. Morphology of the haloarchaeal virus φCh1. (A) Schematic representation of φCh1, featuring an icosahedral head and a contractile tail. (B) Electron micrograph of φCh1 adapted from *(Witte et al., 1997)*.

The virus consists of four major proteins (A, E, H, I) and five minor proteins (B, C, D, F, G), with acidic residues contributing to low isoelectric points similar to those of other halophilic archaea (Lanyi, 1974). The viral genome is partially methylated at adenine residues in the GATC sequence, suggesting the presence of a virus-encoded methyltransferase (Witte *et al.*, 1997). Subsequently, the methyltransferase M. NmaφCh1I was discovered (Baranyi *et al.*, 2000). M. NmaφCh1-I is a Dam-like methyltransferase that is expressed as a late gene, meaning it is produced during the late phase of viral development. Additionally, φCh1 produces two types of tail fiber proteins (gp34 and gp36), with only one, encoded by ORF34, binding to the host *in vitro* (Klein *et al.*, 2012). This virus, adapted to its host's extreme conditions, serves as a model for studying haloalkaliphilic viruses. The genome of φCh1 contains 98 open reading frames (ORFs), with a minimum length of 30 nucleotides. Functional annotation based on sequence similarities identified probable functions for 48 of these ORFs, while many proteins share up to 80% sequence similarity with the φH virus (Klein *et al.*, 2002). As shown in Figure 3, the genome is organized into three functional modules similar to those of tailed, double-stranded DNA bacteriophages like phage λ. The

left part of the genome encodes structural proteins and proteins involved in virion morphogenesis; the central part contains genes for DNA replication, plasmid partitioning and regulation of gene expression; and the right part includes genes of mostly unknown function, along with those involved in DNA modification and restriction (Klein *et al.*, 2002). Some genes are arranged in operons due to overlapping start and stop codons (Klein *et al.*, 2002). Additionally, the mature viral particle contains various host-encoded RNA species ranging from 80 to 700 nucleotides, which are presumed to play a role in viral DNA packaging (Witte *et al.*, 1997).

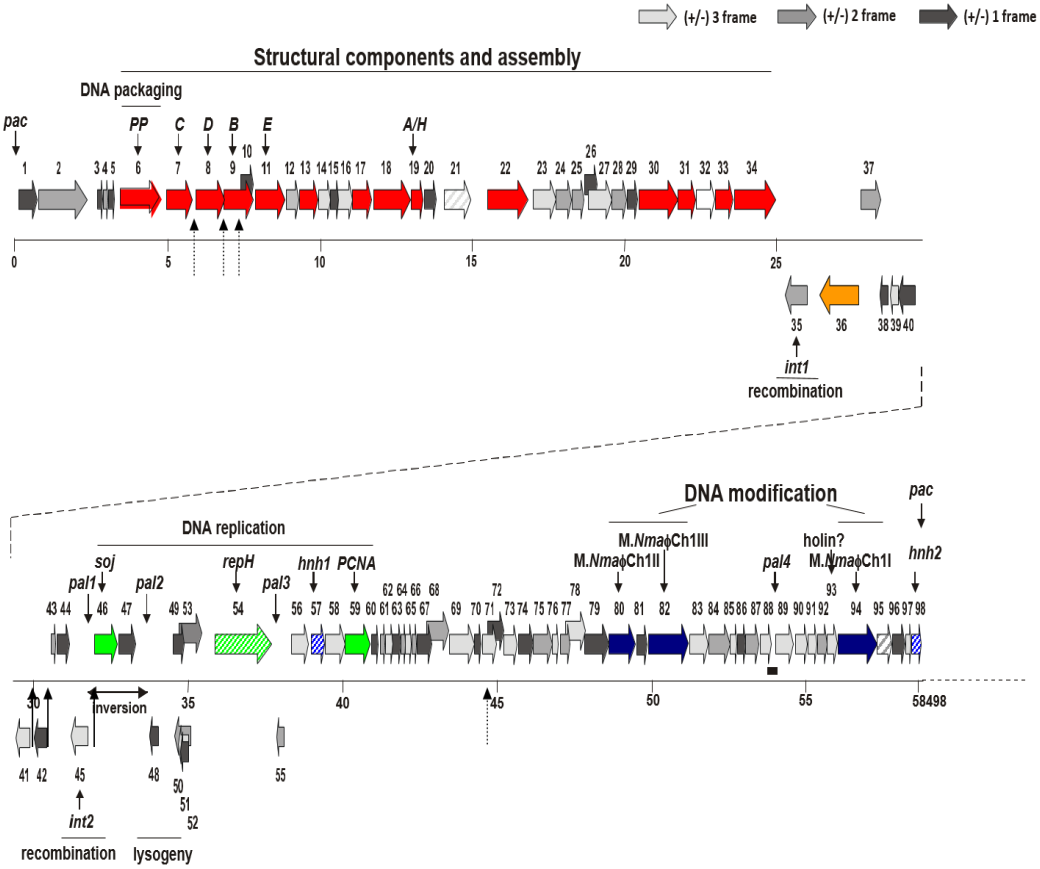

Figure 3. The schematic representation of the φCh1 genome reveals 98 open reading frames (ORFs), depicted as colored arrows. The three shades of grey (light grey, mid-grey, and dark grey) indicate the different reading frames, with arrows showing the orientation of ORFs. The genome is divided into three functional modules responsible for encoding structural components, DNA replication, and DNA modification. Adapted from *(Klein et al., 2002)*.

1.3. Proliferating Cell Nuclear Antigen (PCNA)

Proliferating Cell Nuclear Antigen (PCNA) is a key scaffold protein located at the centre of DNA replication, interacting with a wide variety of partners (Manning *et al.*, 2022a). Acting as a cofactor for DNA polymerases that encircle DNA, PCNA plays a critical role in recruiting essential components to the replication fork. It also regulates the activity of numerous proteins and is crucial for various cellular functions, including cancer genesis (Maga and Hübscher, 2003; Moldovan *et al.*, 2007; Stoimenov and Helleday, 2009).

PCNA forms a trimeric sliding clamp in Eukarya and Archaea, similar to the dimeric β-clamp found in Bacteria (Maga and Hübscher, 2003). The second and third domains of the bacterial β-sliding clamp share sequence homologies with the PCNA proteins of Archaea and Eukarya, suggesting that these proteins originate from a common ancestor and are essential components of the replisome (Arrías *et al.*, 2023). In addition, PCNA also plays significant roles in DNA repair, DNA methylation, chromatin remodelling, and cell cycle regulation (Pan *et al.*, 2011; 2013). All known activities of PCNA proteins require them to encircle the DNA and up to now no enzymatic function has been observed for PCNA when it is not bound to DNA (Pan *et al.*, 2011; 2013).

Proliferating cell nuclear antigen (PCNA) is also crucial in nucleic acid metabolism as a part of the replication and repair machinery. This ring-shaped protein encircles DNA and can slide bidirectionally along the duplex. A key function of PCNA is serving as the processivity factor for DNA polymerases delta and epsilon, anchoring the polymerase to the DNA template for efficient and rapid DNA synthesis. In recent years, it has been found that PCNA interacts with proteins involved in cell cycle progression outside of the DNA polymerase apparatus. Some of these interactions directly impact DNA synthesis, while the roles of others remain unclear (Kelman, 1997).

Immunohistochemical studies have suggested that PCNA is involved in DNA repair. When cells were incubated with anti-PCNA antibodies and exposed to UV light, PCNA was detectable even outside of the S-phase, indicating a role in the DNA repair process. The protein p53, known as the "guardian of the genome," is a key component in the DNA damage response. Increased p53 levels affect the transcription of several genes and cause cell cycle arrest. Cells lacking p53 cannot arrest after DNA damage. It has been shown that p53 acts as a transcriptional activator of the PCNA promoter (Kelman, 1997).

1.4. ORF59 of φCh1

Unusually for a virus, ORF59 of ϕCh1 encodes a putative PCNA, showing high sequence similarity to a putative PCNA produced by the host, which suggests recent horizontal gene transfer (Manning *et al.*, 2022a). Processivity factors are present in less than 20 percent of dsDNA virus genomes, with only a few known in Archaea, making the putative PCNA of ϕCh1 an intriguing target for analysis (Kazlauskas *et al.*, 2016). The ϕCh1 PCNA may act as the processivity factor in ϕCh1 replication by binding to an *N. magadii*-encoded DNA polymerase or to virus-encoded factors specifically required for ϕCh1 replication. It may also interact with the ϕCh1-encoded methyltransferase M. ϕCh1I (Baranyi *et al.*, 2000) and the two additional putative methyltransferases (encoded by ORFs 80 and 82) (R. Klein, U. Baranyi, N. Rössler, B. Greineder, H. Scholz, and A. Witte, 2000). Additionally, ϕCh1 encodes an alternative GUG start codon 63 bp upstream of the primary AUG start codon. In the closely related *Haloferax volcanii*, only 6% of leaderless transcripts, which make up the majority of *H. volcanii* transcripts, use the alternative GUG start codon (Babski *et al.*, 2016). The rare use of the GUG start codon in halophilic Archaea and its potential use by ϕCh1 for an N-terminal extension of the gene encoded by ORF59 relative to the host-encoded homolog makes it an additional investigative target.

1.5. Aim of this study

In prior studies (Manning *et al.*, 2022a) homologous recombination was used to delete the viral PCNA (PCNAϕCh1), demonstrating its significant role in the viral life cycle. The deletion of ORF59 caused a considerable reduction in viral titer, decreased viral protein production, and impaired viral lysis. In addition, complementation and overexpression strains with plasmid expressed viral PCNA variants were generated and analysed for their growth, lytic activity, viral protein production, and virus titer. Complementation and overexpression with wild-type and mutant variants of ORF59 showed that altering the GTG start codon to ATG impacted the viral life cycle, specifically influencing the production of progeny virus particles. The different variants exhibited a wide range of effects on various observed phenotypes. While PCNAϕCh1 was found to be non-essential for the virus, its presence was critical for the efficient production of viral progeny and maintaining the virus-host relationship.

While these previous studies were conducted in L11, the wild-type strain of *N. magadii*, where the effects of viral PCNA were directly assessed, demonstrating the role of the virally encoded PCNA in the virus-host relationship, my aim was to find out how PCNA influences the expression of methyltransferase and gp34 proteins in the L13 cured strain of *N. magadii*, without the virus.

Thus, the central question of this study is: Does PCNA have a direct or indirect effect on the expression of methyltransferase and gp34 proteins in *N. magadii* L13 strain? To address this question, experiments were conducted using *N. magadii* L13, the cured strain lacking the ϕCh1 virus. Three specific PCNA variants were analysed in this study: (1) the wild-type viral PCNA starting with the GTG codon, (2) a variant with the GTG codon changed to ATG, and (3) a truncated version starting with ATG, which is the same size as the host-encoded PCNA.

The experiments were designed to investigate the effect of PCNA on methyltransferase and gp34 protein production in two different systems:

1. In cis: both the PCNA gene and the target gene (gp34) were located on the same genetic element (plasmid), allowing for analysis of direct regulatory or functional interactions.
2. In trans: the PCNA gene and the target gene (ORF94) were placed on two separate plasmids. This approach tested whether PCNA can affect methyltransferase production, and if so, is the effect direct or indirect.

In addition to the wild-type ORF94 construct, a second variant, pNB102-ORF94-M-M1_2, was introduced. This construct contains a mutated upstream region of ORF94 (ORF94-M-M1_2), specifically designed to investigate whether alterations in the upstream regulatory region affect the binding and subsequent expression of the methyltransferase. These strains were then analysed for growth, lytic behaviour and protein expression levels using Western blot.

2. Materials and Methods

2.1. Materials

2.1.1. Strains

Strain	**Genotype**	**Source**
XL1-Blue	*endA*1, *gyrA*96, *hsdR*17 (rk_mK+), *recA*1, *relA*1, supE44, *thi*-1, *lac* [F′, *lacI*q, *lacZ*ΔM15, *proAB*+, Tn10 (TetR)]	Stratagene

N. magadii L11	Wild type strain - φCh1	Witte *et al.*, 1997
N. magadii L13	φCh1 cured strain	Witte *et al.*, 1997

2.1.2. Growth media

2.1.2.1. Natrialba rich medium (NVM)

Components	Amount
Casein hydrolysate	8.8 g
Yeast extract	11.7 g
Tri-sodium citrate dihydrate	0.8
KCl	2.35 g
NaCl	235 g

Adjust pH to 9.5 with NaOH pellets

dd.H_2O ad 935 mL

8 g/L agar for plates

4 g/L agar for top agar

After autoclaving, medium was complemented with:

Components	Volume
0.57 M Na_2CO_3	63 mL
1 M $MgSO_4$	1 mL
20 M $FeSO_4$	1 mL
Trace elements SL-6	1 mL

2.1.2.1.1. 1000 × trace element solution (SL-6)

Components	Amount
$CoCl_2 \times 6H_2O$	0.2 g
$CuCl_2 \times 6H_2O$	10 mg
H_3BO_3	0.3 g
$MnCl_3 \times 4H_2O$	30 mg
$Na_2MoO_4 \times H_2O$	30 mg
$NiCl_2 \times 6H_2O$	20 mg
$ZnSO_4 \times 7H_2O$	0.1 g

dd.H_2O ad 100 mL, autoclave

2.1.2.2. Lysogeny broth (LB)

Components	Amount
Yeast extract	5 g
NaCl	5 g
Peptone	10 g

pH 7.0

dd.H_2O ad 1 L

15 g/L agar for plates

2.1.3. Antibiotics and other additives

Compound	**Stock concentration**	**Final concentration**	**Preparation**
Ampicillin	20 mg/mL	100 µg/mL	dissolved in dd.H_2O, sterile filtered, stored at 4 °C

Chloramphenicol	40 mg/mL	20 µg/mL	dissolved in 96 % EtOH, stored at -20 °C
Tetracycline	10 mg/mL	10 µg/mL	dissolved in half of EtOH and half dd.H_2O, stored at -20 °C
Mevinolin	5 mg/mL	4 µg/mL	Lovastatin Powder dissolved in 96 % EtOH, stored at -20 °C
Novobiocin	3 mg/mL	3 µg/mL	dissolved in dd.H_2O, sterile filtered, storage at -20 °C
Bacitracin	7 mg/mL	70 µg/mL	dissolved in dd.H_2O, sterile filtered, storage at 4 °C
IPTG	1 M	1 mM	dissolved in dd.H_2O, sterile filtered, storage at -20 °C

2.1.4. Plasmids

Plasmid	**Features**	**Source**
pRo-5	bla, ColE1 ori, gyrB (novR), φCh1 derived ori	Mayrhofer-Iro *et al.*, 2013
pRo-5-Mev	*bla*, ColE1 ori, *hmg* (mevR), φCh1-derived ori	Sabic, 2019
pNB102	*bla*, ColE1 ori, *hmg* (mevR), φCh1 derived ori	Zhou *et al.,* 2004
pNB102-ORF94	pNB102 containing ΦCh1 ORF94 (Methyltransferase)	Hofbauer, 2015
pNB102-M-M1_2	pNB102 containing ΦCh1 ORF94 (Methyltransferase), *Eco*RI restriction site introduced into the upstream region	Edwards, 2018
pRo-5-PCNA-GTG-ATG	ΦCh1-ORF59 with a point mutation of GTG>ATG under the control of the promoter	This study

	of ΦCh1-ORF34 in pNB102	
pRo-5-PCNA -Tr	5' truncated ΦCh1-ORF59 under the control of the promoter of ORF34 in pNB102	This study
pRo-5-PCNA-GTG	ΦCh1-ORF59 under the control of the promoter of ΦCh1-ORF34 in pNB102	This study
pNB102-34_{52}	contains $ORF34_{52}$ with its own promoter from plasmid $pBgb34_{52}$	Till, 2010
pRo-5 - $ORF34_{52}$	$ORF34_{52}$ with its own promoter	This study
pKS-34up-PCNA-1VE	5′ truncated ΦCh1-ORF59 under the control of the promoter of ΦCh1-ORF34 in pKSII+	Manning *et al.*, 2022
pKS-34up-PCNA-1ME	ΦCh1-ORF59 with a point mutation of GTG > ATG under the control of the promoter of ΦCh1-ORF34 in pKSII+	Manning *et al.*, 2022
pKS-34up-PCNA-2VE	ϕCh1-ORF59 under the control of the promoter of ϕCh1-ORF34 in pKSII+	Manning *et al.*, 2022
pRo-5-PCNA-Tr-$ORF34_{52}$	5′ truncated ΦCh1-ORF59 under the control of the promoter of ΦCh1-ORF34, $ORF34_{52}$	This study
pRo-5-PCNA-GTG-$ORF34_{52}$	ϕCh1-ORF59 under the control of the promoter of ϕCh1-ORF34, $ORF34_{52}$	This study
pRo-5-PCNA-GTG-ATG_$ORF34_{52}$	ϕCh1-ORF59-GTG changed to ATG under the control of the promoter of ϕCh1-ORF34, $ORF34_{52}$	Ina&Chiara
pRo-5-PCNA-GTG-□ATG-$ORF34_{52}$	ϕCh1-ORF59-GTG, ATG codon 21 changed to CTC, under the control of the promoter of ϕCh1-ORF34, $ORF34_{52}$	Ina&Chiara

2.1.5. Primers

Primer name	Sequence
34-Kpn	CAGCAGGGTACCCGGCGTTCGAGGTCA
PCNA-22	GACAGGTACCTCAGTTGCTCTGGATCCGC
TR-1X	AATTTCTAGACCGCGTTGAAGGCAGCT
TR-2	AAT TTC TAG ATC CTG GGC CTC TTT GAA
N6-541B	CAGGTGATCATGTCCCAGCGCCTCGAG
MT-Xba-3	GATCTCTAGATCACTCATTATCACCGGCGT
MT-Kpn-5	GAATGGTACCGCGAGTCGGACAACGTTC
p30-5	CAGCAGAGATCTATGTTCAAAGCAATCGCTAC
p30-3	CAGCAGAAGCTTTCAGTTGCTCTGGATCCG
34-5	CAGCAGAGATCTATGAGTAAAATCTGGGAACCGAG
36-3	CAGCAGAAGCTTATTCAGGTTTCATGTCGCTG
56-RT5	GAACAGCGCCAGTCCA
56-RT3	GACCACCGGCTTCAGC
34-5-Nde	GCAGCATATGAGTAAAATCTGGGAACCGAG
36-D-5	GACGGGATCCATGGCGGTCGGGAAGT
36-3-Kpn	GCAGGGTACCATTCAGGTTTCATGTCGCTG
pNB102-E-34up	ATCACGAGGCCCTTTCGTCTTCAAGATCGGGTGGGATCCCGACGCGATT
pNB102-E-PCNA-3	TGATAAGCTGTCAAACATGAGAATTTCAGTTGCTCTGGATCCGCGGCGAG

pRo-5-A-34up	GACGTTAGACGCCTCGTGAAGGCACATCGGGTGGGATCCCGACGCGATTT
pRo-5-A-PCNA-3	TAAGCGGGCGTTAATTCGCCCGCACTCAGTTGCTCTGGATCCGCGGCGAG

2.1.6. DNA and protein ladders

DNA ladder	**Size in bp**	**Manufacturer**
GeneRuler 50 bp DNA Ladder	50, 100, 150, 200, 250, 300, 400, 500, 600, 700, 800, 900, 1000	Thermo Scientific
GeneRuler 1 kb DNA Ladder	250, 500, 750, 1000, 1500, 2000, 2500, 3000, 3500, 4000, 5000, 6000, 8000, 10000	Thermo Scientific
GeneRuler 1 kb Plus DNA Ladder	75, 200, 300, 400, 500, 700, 1000, 1500, 2000, 3000, 4000, 5000, 7000, 10000, 20000	Thermo Scientific

Protein ladder	**Size in kDa**	**Company**
PageRuler^{TM} Prestained Protein Ladder	10, 15, 25, 35, 40, 55, 70, 100, 130, 180	Thermo Scientific
PageRuler^{TM} Plus Prestained Protein Ladder	10, 15, 25, 35, 55, 70, 100, 130, 250	Thermo Scientific

2.1.7. Enzymes

Enzyme	Product number	Company
Restriction enzymes	N/A	Thermo Scientific
T4 DNA ligase	M1801	Promega
Fast AP Alkaline Phosphatase	EF0652	Thermo Scientific
2× GoTag Green Master Mix	M7123	Promega
Phusion® Flash PCR Master Mix	F548S/F548L	Thermo Scientific
Lysozyme from chicken egg white	L6876	Sigma
Proteinase K	1019499	Qiagen

2.1.8. Kits

Name	Usage	Company
Promega Wizard® SV Gel and PCR Clean-Up System	Purification of gel-eluted DNA fragments and PCR products	Promega
Wizard® Plus SV Minipreps DNA Purification System	Isolation of plasmid DNA	Promega
Gibson Assembly® HiFi 1-Step Kit	DNA cloning	Synthetic Genomics

2.1.9. Antibodies

2.1.9.1. Primary antibodies

Antibody	Target	Dilution	Source
α- Mtase	Adenine DNA Methyltransferase of φCh1	1:500	Baranyi *et al.*, 2000
α- $gp34_{52}$ (rabbit 20)	Tail fiber protein gp34 of φCh1	1:2500	Till, 2011

All antibodies were produced in rabbits and diluted in 1× TBS, 0.3 % BSA, 0.02 % NaN_3.

2.1.9.2. Secondary antibodies

Antibody	Target	Dilution	Source
ECL™ Anti-Rabbit IgG, HRP linked whole antibody from donkey	Rabbit IgG	1:5000	GE Healthcare

All secondary antibodies were diluted in 1× TBS.

2.1.10. Buffers and solutions

2.1.10.1. Gel electrophoresis

2.1.10.1.1. DNA gels

5×DNA loading dye

Tris.Cl pH 8.2	50 mM
SDS	0.1 % v/v
Bromophenol blue	0.05 % w/v
Xylene cyanol	0.05 % w/v

50× TAE

Tris.Cl pH 8.2	2 M
Acetic acid	1 M
EDTA	0.1 M

0.8 – 1.3 % agarose

Agarose	0.8 – 1.3 g
in 100 mL 1× TAE	

Ethidium bromide bath

Ethidium bromide	10 µg/mL
in 1000 mL H_2O	

50× Superbuffer

NaOH	0.5 M
Boric Acid	1.82 M

2.1.10.1.2. Protein gels

2×Laemmli buffer

Tris.Cl pH 6.8	125 mM
SDS	4 % v/v
β-mercaptoethanol	10 % v/v
Glycerol	20 % v/v
Bromphenol blue	0.04 % w/v

5 mM sodium phosphate buffer

Na_2HPO_4	1 M
NaH_2PO_4	1 M
pH 6.8	

30 % acrylamide solution (29:1)	
Acrylamide	73 g
N, N'-	
methylene-bisacrylamide	2 g
dd.H_2O ad 250 mL and filter	

10× SDS Running buffer	
Tris	250 mM
Glycine	1.92 M
SDS	1 % w/v

Stacking gel buffer	
Tris.Cl pH 6.8	0.5 M
SDS	0.4 % v/v

Separating gel buffer	
Tris.Cl pH 8.8	1.5 M
SDS	0.4 % v/v

Coomassie staining solution	
Methanol	25 % v/v
Acetic acid	10 % v/v
Coomassie Brillant	
Blue R250	0.25 % w/v

Destaining solution	
Acetic acid	10 % v/v

2.1.10.2. Gibson assembly

5× ISO buffer	
Tric.Cl pH 7.5	500 mM
DL-Dithiothreitol	50 mM
dATP, dCTP,	
dGTP, dTTP	1 mM
NAD	5 mM
PEG-6000	25 % w/v

2× Gibson Assembly Master Mix	
5×ISO buffer	320 µL
Phusion polymerase	20 µL
T5 Exonuclease	1.5 µL
Taq DNA ligase	160 µL
dd.H_2O ad 1 mL	

2.1.10.3. Western Blot

10×TBS

Tris.Cl pH 8.0	250 mM
NaCl	1.37 M

1×Towbin transfer buffer

Tris	25 mM
Glycine	192 mM
Methanol	20 % v/v

Ponceau-S staining solution

Ponceau-S	0.5 % w/v
Trichloracetic acid	3 % v/v

Blocking solution

Skim milk powder	5 % w/v
in 1×TBS	

Coumaric acid solution

Coumaric acid	0.148 g
DMSO	10 mL

Luminol solution

Luminol	0.886 g
DMSO	20 mL

ECL buffer

1.5 M Tris.Cl pH 8.5	13.3 mL
Luminol	500 µL
Coumaric acid	250 µL
dd.H_2O ad 200 mL	

Membrane stripping buffer

1 M Tris.Cl pH 6.8	30 mL
β-mercaptoethanol	3.95 mL
SDS	2 % v/v
dd.H_2O ad 500 mL	

2.1.10.4. Preparation of competent cells

2.1.10.4.1. Buffers for the generation of *E. coli* competent cells

MOPS I		MOPS II	
MOPS	100 mM	MOPS	100 mM
KCl	10 mM	KCl	10 mM
RbCl	10 mM	RbCl	10 mM
pH 7		pH 6.5	

MOPS IIa

MOPS	100 mM
KCl	10 mM
RbCl	10 mM
Glycerol	15 % v/v

pH 6.5

pH was adjusted with KOH

2.1.10.4.2. Buffers for the generation of *N. magadii* competent cells

Buffered high salt spheroplasting solution

NaCl	2 M
KCl	27 mM
Tris.Cl pH 9.5	50 mM

After autoclaving: add 15 % v/v sucrose (sterilized by filtration)

Unbuffered high salt spheroplasting solution (UBSS-HS)

NaCl	2 M
KCl	27 mM

After autoclaving: add 15 % v/v sucrose (sterilized by filtration)

60 % PEG 600		0.5 M EDTA	
PEG 600	60 % v/v	EDTA	0.5 M
UBSS-HS	40 % v/v	pH 8 (adjusted with NaOH pellets)	
pH 5.9		pH 4.5	

2.2. Methods

2.2.1. DNA methods

2.2.1.1. Preparation of DNA templates and primers

N. magadii DNA templates were prepared by centrifuging 30 µL culture at 13000 rpm for 3 min at RT followed by resuspension of the pellet in 100 µL dd.H_2O. 1 µL of cell suspension was used directly as template for PCR.

For *E. coli* overnight cultures, 1µl of the culture was used directly as a DNA template.

All primers used in this study were delivered in a lyophilized state. The stock primers were reconstituted in dd.H_2O to a concentration of 1µg/µL. Prior to the PCR reaction the primers were diluted 1:10.

The annealing temperatures were estimated by using the TM Calculator from Thermo Scientific website or alternatively NEB TM Calculator.

2.2.1.2. PCR Reactions

2.2.1.2.1. Preparative PCR

For preparative PCR reactions the Phusion Hifi© polymerase was used. This polymerase has a 3'→5' exonuclease activity (proofreading) and therefore allows a reliable amplification of the desired PCR product.

Component	**Volume**
DNA template	1 µL
Forward primer	2.5 µL
Reverse primer	2.5 µL
Phusion® Flash PCR Master Mix	25 µL
dd.H_2O	ad 50 µL

Step	**Temperature (°C)**	**Time (mm:ss)**
Initial Denaturation	98	03:00 - 05:00
Denaturation	98	00:10
Annealing	Tm primer – 4 °C	00:07
Elongation	72	15 sec/ 1 kbp
Final Elongation	72	05:00
Hold	16	∞

2.2.1.2.2. Analytical PCR

For all analytical PCR reactions, Taq polymerase was used. The *Taq* polymerase is part of the GoTaq© Master Mix, which has also the loading dye incorporated.

Component	**Volume**
DNA template	1 µL
Forward primer	1.5 µL
Reverse primer	1.5 µL
GoTaq© Master Mix	12.5 µL
ddH_2O	ad 25 µL

Step	**Temperature (°C)**	**Time (mm:ss)**
Initial Denaturation	95	05:00
Denaturation	95	00:10
Annealing	Tm primer – 4 °C	00:07
Elongation	72	1min/ 1kbp
Final Elongation	72	05:00
Hold	16	∞

2.2.1.3. Quality control and purification of the PCR products

In order to analyze and verify the DNA amplicon, ensure its specificity and determine product size, 5 µL of the PCR reaction was mixed 1:1 with 5 µL of 5× DNA loading dye and was loaded on an 0.8 % agarose gel. The gel was stained with EtBr for approximately 10 minutes and visualized with UV light in the ChemiDoc XRS+ apparatus.

For analytical PCR products no addition of DNA loading dye was needed because the *Taq* polymerase mixture contains the loading dye.

PCR products and plasmid DNA were purified using Wizard® SV Gel and PCR Clean-up System and Wizard®Plus SV Minipreps DNA Purification System. The concentration of the purified DNA was measured by Nanodrop (ND-2000c, Thermo Scientific) and the ratio of absorbance at 260 nm and 280 nm was used to assess the DNA purity. A 260/280 ratio of ~1.8 was generally accepted as "pure".

2.2.1.4. DNA restriction and dephosphorylation

All restrictions were performed using restriction enzymes and buffers from Thermo Scientific according to the manufacturer's instructions. The restriction was performed at 37 °C overnight, followed by quality assessment on an 0.8 % agarose gel. The unrestricted plasmid was loaded as a control.

Furthermore, plasmid DNA was additionally dephosphorylated in order to prevent re-circularization. The reaction was incubated 30 min at 37 °C, followed by thermal inactivation of the alkaline phosphatase at 65 °C for 15 min. Prior to ligation, plasmid DNA was purified (see Section 2.2.1.3.).

2.2.1.5. DNA ligation

The ligation was performed by using T4 DNA ligase according to the manufacturer's instructions. Molar ratios of vector to insert, 1:3 to 1:9, were used and the assay was incubated either for 3 hours at RT or overnight at 16 °C.

2.2.1.6. Gibson assembly

Gibson Assembly is a revolutionary cloning method that allows joining of multiple DNA fragments, without the need for traditional restriction enzymes and ligation steps.

In this study plasmid DNA was linearized, purified and then mixed with the fragments of interest (0.5 – 1 pmol per fragment) and 10 µL of 2x Gibson Assembly master mix. The mixture was incubated at 50 °C for 15 min. For transformation into *E.coli* XL1-Blue 10 µL of the assembly was used.

2.2.2. Transformation procedures

2.2.2.1. Transformation in *E. coli*

2.2.2.1.1. Generation of *E. coli* competent cells

For the preparation of XL1-Blue competent cells an overnight preculture was inoculated in 200 mL LB medium, supplemented with tetracycline, with a starting OD_{600} of 0.1. The culture was incubated at 37 °C under agitation until an OD_{600} of 0.6 was reached. Cells were then harvested by centrifugation at 10000 rpm for 10 min at 4 °C and the pellet was resuspended in 80 mL MOPS I and incubated on ice for 10 minutes. Afterwards cells were collected by a second centrifugation step at 10000 rpm for 10 min at 4 °C, followed by the resuspension of the pellet in 80 mL MOPS II and incubation on ice for 30 min. After the third and final centrifugation step the pellet was resuspended in 4 mL MOPS IIa and stored at -80 °C in 100 µl aliquots.

2.2.2.1.2. *E. coli* transformation

For the transformation assay 15 µL of the ligation reaction or 10 µL of Gibson Assembly was added into 100 µL freshly thawed XL1-Blue competent cells. The mixture was incubated on ice for 30 min, followed by heat shock at 42 °C for 2 minutes and then immediately cooled

on ice. 300 µL LB was added and the cells were regenerated at 37 °C for 30 min under agitation. The transformation assay was plated on LB plates with antibiotics (amp/ tet) and incubated overnight at 37 °C.

Single colonies were picked and inoculated in 5 mL LB (amp/ tet) for overnight growth. The clones were tested by analytical PCR. The DNA of putative positive clones was isolated and sent for sequencing (Microsynth).

2.2.2.2. *N. magadii* Transformation

2.2.2.2.1. Generation of *N. magadii* competent cells

To produce *N. magadii* competent cells, an overnight culture of *N. magadii* was inoculated in 50 mL NVM+ medium with bacitracin at a final concentration of 70 µg/mL. The culture was grown until an OD_{600} between 0.6 and 1 was reached. The cells were then collected by centrifugation at 6000 rpm for 15 minutes at room temperature. The cell pellet was subsequently resuspended in 30 mL of a buffered high-salt spheroblasting solution. Proteinase K was added to the suspension to a final concentration of 0.1 % v/v. The cell mixture was incubated at 42 °C with shaking for two days, during which spheroblast formation was monitored under a microscope.

2.2.2.2.2. Transformation of *N. magadii* competent cells and screening

1.5 ml of freshly prepared *N. magadii* competent cells were centrifuged at 10000 rpm for 5 minutes at room temperature. The resulting pellet was resuspended in 150 µL of buffered high-salt spheroblasting solution, followed by the addition of the DNA of interest (1-3 µg; maximum 10 µL) and incubation for 5 minutes at RT. 150 µL of 60 % PEG-600 (in HS unbuffered spheroplasting solution) was added to the transformation mix and incubated 20 to 30 minutes. Removal of PEG-600 residues was achieved by washing the cell mixture twice

with 1 ml NVM CAA+ (10000 rpm, 5 minutes, RT). The final pellet was resuspended in 1 ml NVM CAA+ and incubated at 37 °C with agitation for two to three days until the cells were regenerated; switch from spheroplasts to their original rod shaped morphology. Finally, 100 µL of the cell suspension (undiluted, 1:10 and 1:100 dilution) was plated on NVM CAA+ agar plates with antibiotics and incubated at 42 °C. Single colonies were inoculated in 500 µL NVM CAA+ with antibiotics and incubated at 37 °C under agitation, followed by screening with analytical PCR as stated on section 2.2.1.2.2.

2.2.3. Protein methods

2.2.3.1. Preparation of crude protein extracts

Protein crude extracts were taken daily for one week and were used to analyze proteins from *N. magadii.* 1.5 ml of cell culture was centrifuged at 13000 rpm for 3 minutes at room temperature. The pellet was resuspended in equal volumes of 5 mM sodium phosphate buffer pH 6.8 and 2× Laemmli buffer. The amount of phosphate and Laemmli buffer was calculated based on the formula OD_{600} × 75. *N. magadii* protein extracts were incubated at 37 °C until complete dissolution of the pellet was achieved, followed by denaturation for 10 minutes at 95 °C and storage at -20 °C.

E. coli protein extracts were immediately denatured and stored at -20 °C.

2.2.3.2. SDS-PAGE and Coomassie staining

SDS-Polyacrylamide Gel Electrophoresis (SDS-PAGE) was used to separate the proteins in the crude extracts of *Natrialba magadii* based on their molecular weights.10 µL of each sample was applied to a discontinuous SDS-PAGE system, comprising a 12 % resolving gel and a 4 % stacking gel. Due to the high salt content in the protein extracts of *N.magadii*, the

gel was run slowly for 4-5 hours at reduced voltage (40 V). Bacterial proteins were fractioned at 40 V until the samples reached the end of the stacking gel. Upon entry into the resolving gel, the voltage was increased to 60 V and separation of the proteins was continued until the bromphenol blue dye reached the bottom of the gel. The procedure was carried out using a BioRad Mini Protean apparatus with 1× SDS running buffer. After electrophoresis, the gel was stained with Coomassie staining solution for 5-10 minutes, followed by overnight incubation in destaining solution under constant agitation.

2.2.3.3. Western Blot

Western blot was used to detect and analyze specific proteins by firstly separating them via 12 % SDS-PAGE and subsequent transfer to a nitrocellulose membrane (9 × 6 cm; GE Healthcare Amersham™ Protran™ 0.2 µm NC) via a semi-dry method.

Within the Trans-Blot® Turbo™ Transfer System from BioRad, a "sandwich" was assembled consisting of three Whatman papers, the nitrocellulose membrane, the SDS-Gel, and three additional Whatman papers. The Whatman papers and the nitrocellulose membrane were soaked in 1× transfer buffer. To remove any trapped air bubbles and excess liquid between the layers, a tube was rolled gently over the "sandwich" and dabbed off any remaining moisture. The blotting was conducted at 25 mA for 30 minutes. To confirm the successful transfer to the nitrocellulose membrane, the membrane was quickly stained with Ponceau S solution. The Ponceau S solution was removed by washing with tap water. After the transfer, the marker lines on the membrane were traced with an indelible pen for easier visualization later. The membrane was then blocked overnight at 4 °C in a 5 % milk powder solution.

The next day the membrane was washed three times with 1× TBS for 10 minutes, followed by incubation with 10 mL of primary antibody solution for one hour shaking at room

temperature. Upon binding of the primary antibody, the membrane was washed three times with 1× TBS for 10 minutes and then the horseradish peroxidase-conjugated anti-rabbit Ig secondary antibody was added to the membrane and incubated at room temperature for one hour. The membrane was further washed with 1× TBS.

For detection 3 mL ECL and 3 µL H_2O_2 were added to the membrane and detection was achieved by the ChemiDoc XRS+ imager and ImageLab software, with exposure time varying from five to 180 seconds. In addition, a colorimetric picture was taken to visualize the marker.

In case that it was necessary to re-develop the same membrane with a different primary antibody, the membrane was stripped. Membranes were stripped by washing three times with 1× TBS at room temperature and subsequent addition of 10 mL ROTI®Free Stripping Buffer (Roth), followed by incubation for 30 minutes at 37 °C. The stripping buffer was removed by extensive washing with 1× TBS and membranes were re-blocked overnight.

2.2.4. Cloning strategies

2.2.4.1. Transformation of PCNA variants into L13 *N. magadii*

2.2.4.1.2. Co-transformation assay

For the co-transformation assay, *N. magadii* L13 was transformed with two shuttle vectors. The first, pRo-5, contained one of three PCNA variants: pRo-5-34up-PCNA_GTG-ATG, where the GTG start codon was changed to ATG; pRo-5-34up-PCNA_Tr, a truncated version with ATG as the start codon; and pRo-5-34up-PCNA_WT, the wild-type viral PCNA with the original GTG start codon, constructed by Witte *et al.*, (2022). An empty pRo-5 vector was used as a control. The second vector, pNB102, contained ORF94 with its native promoter sequence, constructed by Haider, 2014. The resulting clones were screened for the insert of both plasmids and were used to analyse the effect of PCNA on methyltransferase expression.

In, addition, pNB102 plasmid containing the mutated upstream region of ORF94 (ORF94-M-M1_2) constructed by (Edwards, 2018), was co-transformed into *N. magadii* L13 with each of the three PCNA variants to evaluate the effect of PCNA on methyltransferase expression.

2.2.4.1.3. Transformation assay

The pRo-5 plasmid, containing one of three variants of PCNA (as described above) under the control of the ORF34 promoter, was transformed into *N. magadii* L13 to assess the influence of PCNA on gp34 expression.

2.2.4.2. PCNA constructs via Gibson Assembly

2.2.4.2.1. pNB102-ORF34-PCNA variants constructs via Gibson Assembly

pNB102-ORF34$_{52}$ was restricted with *Eco*RI and *Pm*lI. PCR fragments were amplified with pNB102-N-34up and pNB102-E-PCNA-3 primers.

Table 1. Construction of pNB102-PCNA variants via Gibson assembly.

Fragment	**Primer 1**	**Primer 2**	**Template**	**Fragment size**
pNB102-ORF34$_{52}$				
PCNA truncated	pNB102-N-34up	pNB102-E-PCNA-3	φCH1	1049 bp
PCNA truncated valine for methionine	pNB102-N-34up	pNB102-E-PCNA-3	φCH1	1112 bp
PCNA Original	pNB102-N-34up	pNB102-E-PCNA-3	φCH1	1112 bp

2.2.4.2.2. pRo5-ORF34$_{52}$-PCNA variants constructs via Gibson Assembly

pRo5-ORF34$_{52}$ was restricted with *Pml*I (*Acv*I). PCR fragments were amplified with pRo-5-A-34up and pRo-5-A-PCNA-3. Both vector and fragment were excised from the gel and purified using a commercial kit. The DNA concentration was measured via Nanodrop and Gibson Assembly was performed.

Table 2. Construction of pRo5-PCNA variants via Gibson Assembly

Fragment	**Primer 1**	**Primer 2**	**Template**	**Fragment size**
PCNA truncated	pRo-5-A-34up	pRo-5-A-PCNA-3	φCH1	1049 bp
PCNA, valine codon changed to methionine codon	pRo-5-A-34up	pRo-5-A-PCNA-3	φCH1	1112 bp
PCNA wild type	pRo-5-A-34up	pRo-5-A-PCNA-3	φCH1	1112 bp

2.2.4.2.3. Construction of pRo-5 - ORF34$_{52}$

ORF34$_{52}$ was amplified with primers 34-Kpn and 36-3 using plasmid pBgB52 as a template. pRo-5 as well as the PCR fragment were restricted with *Kpn*I and *Hind*III and ligated. After screening the plasmid was send for sequencing.

3. Results and Discussion

The focus of this study is the Proliferating Cell Nuclear Antigen (PCNA), a pivotal scaffold protein primarily involved in DNA replication, which interacts with numerous proteins essential for cellular processes (Manning, *et al.* 2022). Remarkably, the virus ϕCh1 encodes a putative PCNA, a rare occurrence for viral genomes. Its host, *N. magadii*, similarly encodes a PCNA with high sequence similarity to the viral counterpart, differing by an alternative GUG start codon upstream of the conventional AUG. This results in a longer protein product in *Natrialba magadii.*

In order to investigate the effect of PCNA on the production of methyltransferase and gp34 proteins, experiments were conducted using two different systems. In the cis system, both the PCNA gene and the target gene for gp34 expression were located on the same genetic element, facilitating the analysis of direct regulatory or functional interactions. Meanwhile, in the trans system, the PCNA gene and the target gene (ORF94) were placed on separate plasmids, allowing us to assess whether PCNA influences methyltransferase production and, if so, whether the effect is direct or indirect.

Various PCNA variants were constructed and used for the experiments: (1) the wild-type ϕCh1 PCNA starting with codon GTG, (2) a mutant where GTG codon is changed to ATG, and (3) a truncated version starting with ATG, matching the size of the host-encoded PCNA. These strains were then analysed for growth, lytic behaviour, and viral protein levels using Western blot.

Table 3. Strains created for the analysis of $PCNA_{\Phi Ch1}$. Features: [1]: wild type PCNA starting with codon GTG, [2]: changed GTG codon to ATG, [3]: truncated version starting with ATG, same size as the host encoded PCNA. N_{60} represents the 60 nucleotides between the GTG and the ATG, [4]: Change of the ATG codon to CTC (Manning *et al*, 2022, with modifications).

Strains	
Overexpression	**Feature**
N. magadii L13 (pNB102)	Control
N. magadii L13 (pNB102-PCNA-GTG)	GTG-N_{60}-ATG[1]
N. magadii L13 (pNB102-PCNA-ATG)	ATG-N_{60}-ATG[2]
N. magadii L13 (pNB102-PCNA-Tr)	ATG[3]
N. magadii L13 (pNB102-PCNA-ATG-□ATG)	ATG-N_{60}-□ATG[4]
N. magadii L13 (pNB102-PCNA-GTG_□ATG)	GTG-N_{60}-□ATG[4]

3.1. Effect of PCNA on the methyltransferase expression in *N. magadii*

Since PCNA is known to interact with other proteins involved in DNA replication and repair (Pan *et al.*, 2011), it may influence the expression or activity of ORF94-encoded methyltransferase. To investigate the effect of PCNA in methyltransferase expression, a co-transformation assay into *N. magadii* L13 was performed. Co-transforming ensures that both the methyltransferase and PCNA are present in the same cells, allowing to observe any functional or regulatory effects PCNA might have on methyltransferase production.

As shown in Figure 4, two shuttle vectors, pNB102 and pRo-5, were used for the co-transformation assay. The pNB102 plasmid, containing ORF94 with its own promoter sequence was co-transformed with pRo-5 plasmid containing one of three variants of PCNA ϕCh1 under the control of the ORF34 promoter.

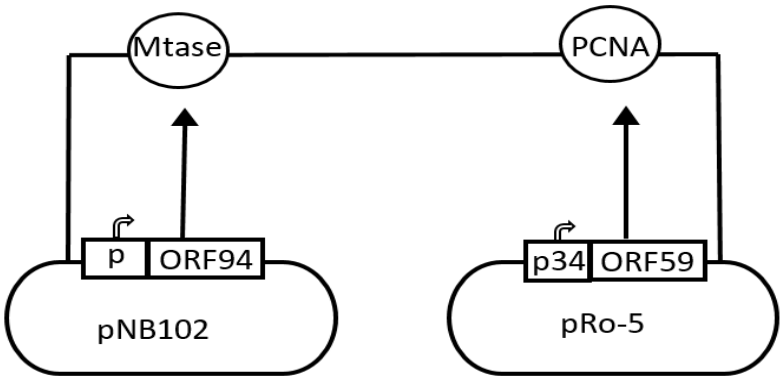

Figure 4. Schematic illustration of plasmids used for the co-transformation assay including pNB102 plasmid, containing ORF94 with its own promoter sequence and the pRo-5 plasmid containing one of three variants of PCNA ϕCh1 under the control of the ORF34 promoter.

Empty plasmid controls were also introduced in the experiment and these constructs were co-transformed via PEG-600 mediated transformation assay. Positive colonies were identified using colony PCR (Figure 5).

A) B)

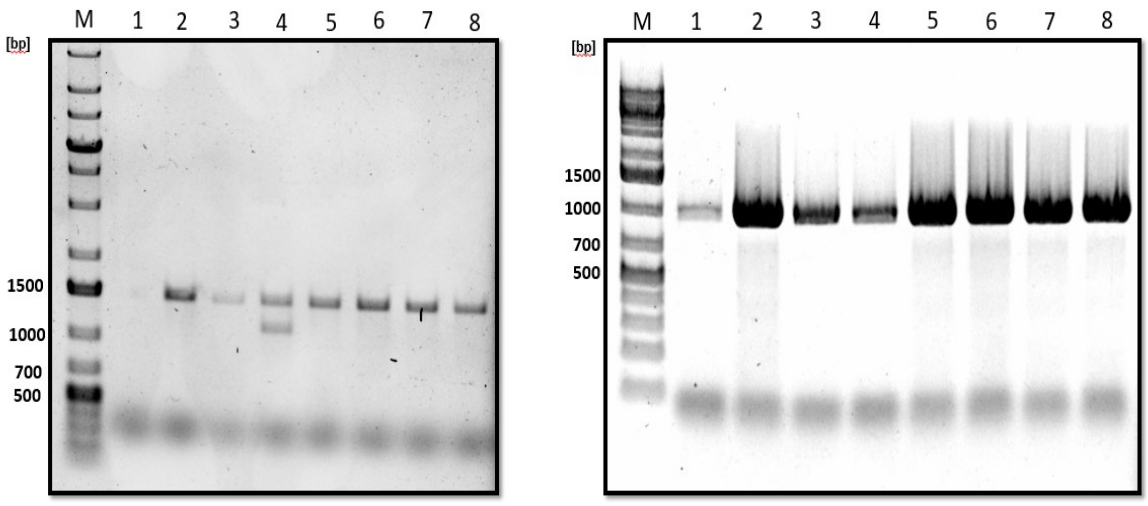

Figure 5. Agarose gel electrophoresis analysis of colony PCR screening for positive transformants.

A) Colony PCR screening for the insert of pNB102 plasmid. Lane 1: 1-kb+-ladder, Lane 1-4 truncated PCNA, lane 5-8 wild-type PCNA.

B) Colony PCR screening for the insert of pRo-5. Lane 1: 1-kb+-ladder, lane1-4: truncated PCNA, lane 5-8: wild-type PCNA.

Successful *N. magadii* L13 transformants were inoculated into NVM/CAA+ medium with the corresponding antibiotic. Liquid pre-cultures were initially prepared and incubated at 42 °C under constant agitation to promote growth. These pre-cultures were monitored until they reached an OD_{600} value of at least 0.3, indicating sufficient cell density. Once this threshold was met, fresh liquid cultures were inoculated at a lower seeding density of 0.1 and then incubated at 37 °C on a shaker to maintain consistent agitating. Clones of each strain were selected and analysed over the course of 7 days (168 hours) to study their growth kinetics. OD_{600} measurements were taken at regular 24-hour intervals to track the growth dynamics, while samples were also collected at each time point for further Western blot analysis.

3.1.1. Growth kinetics analysis of N. magadii L13 strains expressing the methyltransferase

OD_{600} measurements of each clone were taken at regular 24-hour intervals to track the growth dynamics and generate growth curves. Unfortunately, the PCNA variant containing the GTG codon changed to ATG did not exhibit growth under the experimental conditions. As a result, growth curve data and Western blot analysis for this construct could not be obtained.

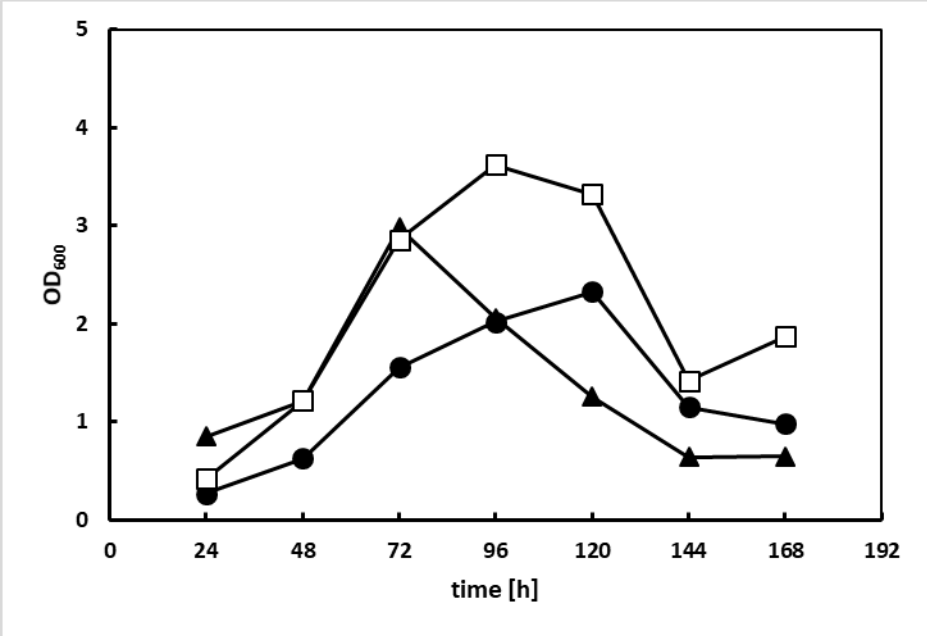

Figure 6. Growth kinetics of *N. magadii* L13 PCNA constructs including truncated version (pRo-5-PCNA-Tr) (●), wild-type version (pRo-5-PCNA-GTG) (▲) and the control (pRo-5) *(❐)* over the course of 7 days (168 hours). Strains were inoculated in NVM/CAA+ medium with the corresponding antibiotic, with an optical density of 0. 1 and grown at 37 °C with agitation. The optical densities were measured at 600 nm and measurements were taken at regular 24-hour intervals.

Figure 6 shows that the truncated strain of PCNA showed a decreased optical density at day 5, exhibiting similar growth behaviours to the control strain, which also initiated decreased optical density at day 5 after inoculation. Both strains show notably different growth patterns compared to the wild-type strain, which begins lysis between day 3 and day 4 after

inoculation. This variation in lysis timing highlights the differences in how these PCNA variants affect cellular stability and growth. The earlier onset of lysis in the wild-type strain suggests a different regulatory or functional role compared to the truncated and control strains. Understanding these lysis patterns provides a baseline for assessing the effects of PCNA variants on protein expression.

3.1.2. Western blot analysis of methyltransferase production

Western blot analysis was performed to further investigate the expression of methyltransferase (encoded by ORF94) in the presence of different PCNA variants in *N. magadii* L13, and to understand whether PCNA exerts a direct or indirect effect on the production of methyltransferase. Western blot analyses were done using whole cell extracts prepared from samples taken every 24 hours for seven days from *N. magadii* L13 cultures cultivated in NVM+ medium. In addition, whole cell extracts prepared from *N. magadii* L11 and *N. magadii* L13 were used as positive and negative control respectively. Polyclonal rabbit antibody was prepared against the methyltransferase protein.

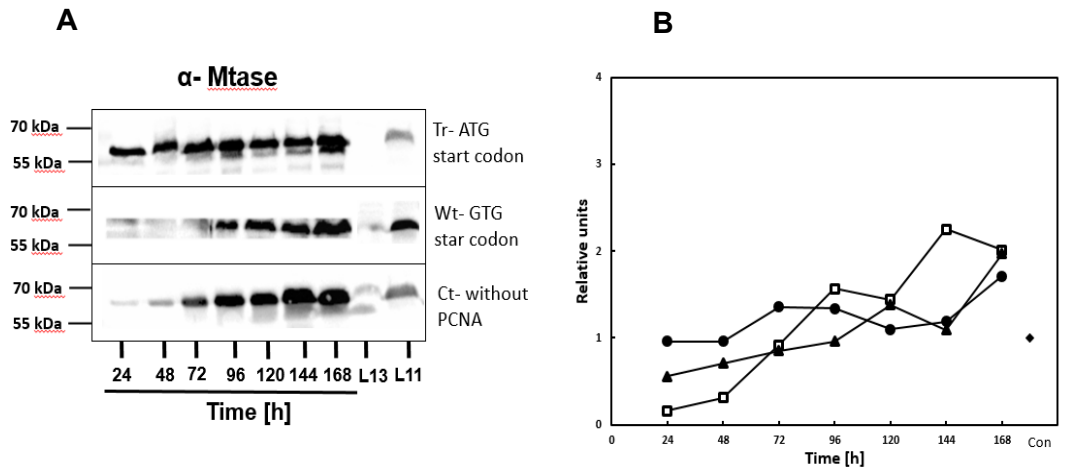

Figure 7. A: Western blot analysis of *N. magadii* L13 PCNA constructs including truncated version (pRo-5-PCNA-Tr), wild-type version (pRo-5-PCNA-GTG) and the control (pRo-5) with antibody against Mtase. Marker: PageRuler™ Plus Prestained Protein Ladder, 10 to 250 kDa; lane 1-7 (left to right): samples from day 1-7; *N. magadii* L13 negative control; *N. magadii* L11 positive control). Protein sizes are indicated on the left. B**:** Protein levels of the of N. magadii L13 PCNA strains including truncated version (pRo-5-PCNA_Tr) (●), wild-type version (pRo-5-PCNA_WT) (▲) and the control (pRo-5) (❒) as measured by Western blot and analyzed. In addition, L11 cell extract was used a positive control (◆) and set as 1. Densitometry analyses were done using Image lab tool from BioRad.

The wild-type PCNA variant shows low initial production of methyltransferase as indicated by faint bands in the first 72 hours. However, a significant increase in intensity is observed after 72 hours, suggesting that the protein expression becomes more robust beyond this point. The bands continue to intensify over time, reaching their peak expression between 120 and 144 hours (Figure 7). Despite the slightly delayed onset, this time-dependent increase in methyltransferase production suggests that wild-type PCNA plays a role in enhancing protein synthesis.

In contrast to the wild-type, the truncated version of PCNA shows a much earlier onset of methyltransferase production. Clear bands are already visible at 24 hours. As the time progresses, the bands grow steadily more intense, reflecting consistent and increasing methyltransferase production over the course of the experiment.

The early appearance of the bands suggests that truncated PCNA can activate the production machinery more quickly than the wild-type variant. However, even though the expression begins earlier, the intensity does not reach the same peak levels as the wild type in later time points.

This could imply that while the truncated form initiates production earlier, it might not sustain the same level of protein synthesis over time.

In the control construct, which lacks a functional PCNA, there is a gradual increase in methyltransferase production. Weak bands begin to appear between 24 and 48 hours, showing that the cells still produce methyltransferase, though at lower levels.

The intensity of the bands increases steadily but more slowly than in the truncated and wild-type PCNA variants, with the highest levels observed between 120 and 168 hours.

The slow and steady increase in the control construct suggests that, without PCNA, cells can still produce methyltransferase.

3.2. Effect of PCNA on the upstream-mutant methyltransferase

In addition to the wild-type ORF94 construct, a second variant, pNB102-ORF94-M-M1_2, was introduced. This construct contains a mutated upstream region of ORF94 (ORF94-M-M1_2), specifically designed to investigate whether alterations in the upstream regulatory region affect the binding and subsequent expression of the methyltransferase.

The same two shuttle vectors, pNB102 and pRo-5, were used for the double transformation assay into *N. magadii* L13. The pNB102 plasmid, containing the mutation on the upstream region of ORF94 with its own promoter sequence was co-transformed with pRo-5 plasmid containing one of three variants of PCNA ϕCh1 under the control of the ORF34 promoter, as seen in Figure 8.

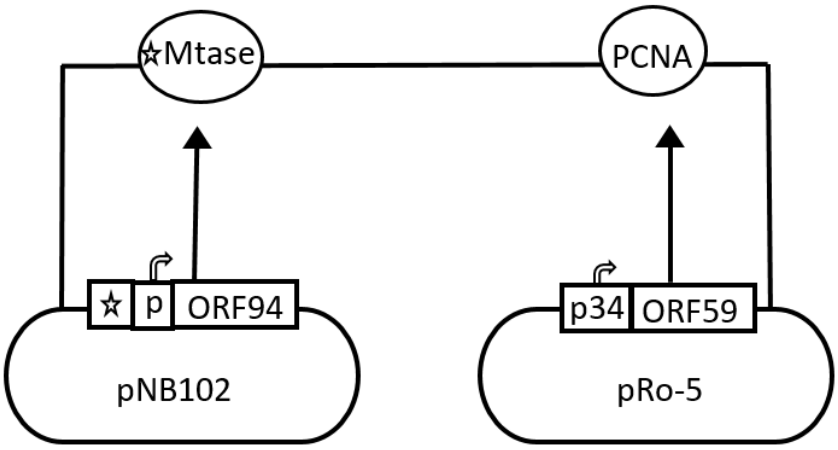

Figure 8. Schematic illustration of plasmids used for the co-transformation assay into *N. magadii* L13 including pNB102 plasmid, containing a mutation on the upstream region of ORF94 with its own promoter sequence and the pRo-5 plasmid containing one of three variants of PCNA ϕCh1 under the control of the ORF34 promoter.

Empty plasmid controls were also introduced as part of the experimental design to serve as a baseline for comparison. These control constructs, alongside the experimental plasmids, were co-transformed into *N. magadii* L13 strain, using a PEG-600-mediated transformation assay. The purpose of including these empty plasmids was to rule out any non-specific effects that might arise from the transformation process itself, ensuring that any observed effects were due to the presence of the plasmid-encoded genes of interest. Following the transformation, positive colonies were identified through colony PCR, which confirmed the successful integration of the plasmids into the host cells (Figure 9).

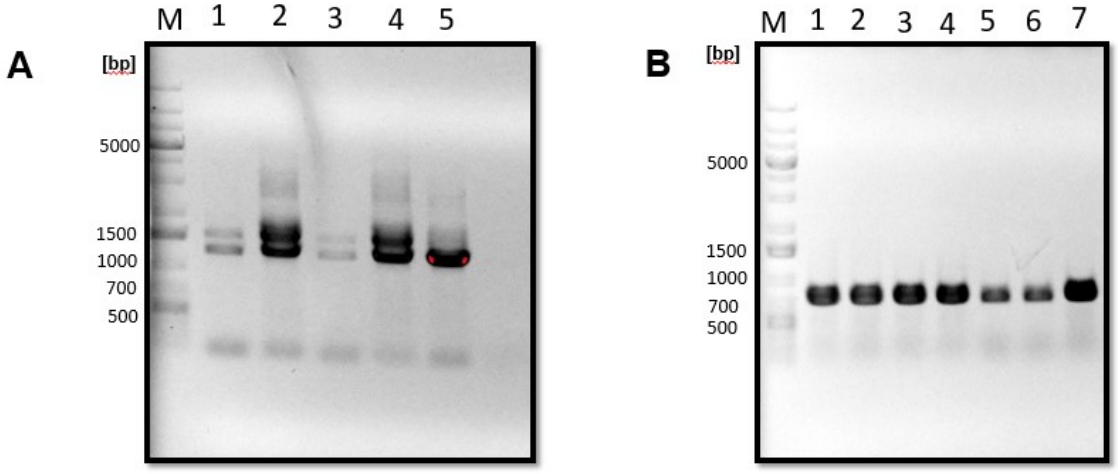

Figure 9. Agarose gel electrophoresis analysis of colony PCR screening of positive transformants.

A) Colony PCR screening for the insert of pNB102 plasmid. Lane 1: 1-kb+-ladder, Lane 1-5 truncated PCNA.

B) Colony PCR screening for the insert of pRo-5. Lane 1: 1-kb+-ladder, lane1-7: truncated PCNA.

Successful *N. magadii* L13 transformants were inoculated into NVM/CAA+ medium containing the appropriate antibiotic. Initial liquid pre-cultures were prepared and incubated at 42 °C with constant agitation to facilitate cell growth. These pre-cultures were monitored until they reached an OD_{600} of at least 0.3, signifying adequate cell density. At that point, new liquid cultures were prepared at a lower starting concentration of 0.1 OD_{600} and incubated at 37 °C under shaking conditions to ensure continuous agitation. Clones from each strain were selected and monitored over a 7-day period (168 hours) to generate growth curves.

3.2.1. Growth kinetics analysis of N. magadii strains expressing the methyltransferase

OD_{600} measurements of each clone were taken at regular 24-hour intervals to track the growth dynamics and generate growth curves. Unfortunately, the PCNA variants containing the GTG codon changed to ATG, and the wild-type did not exhibit growth under the experimental conditions. As a result, growth curve data and Western blot analysis for these constructs could not be obtained.

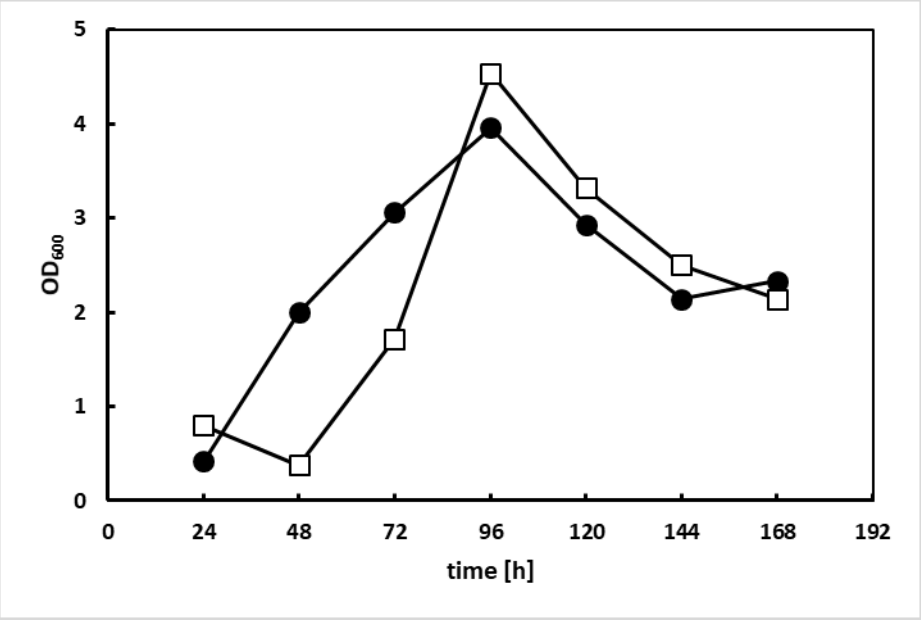

Figure 10. Growth kinetics of *N. magadii* L13 PCNA constructs including truncated version (pRo-5-PCNA-Tr) (●) and the control (pRo-5) (❐) over the course of 7 days (168 hours). Strains were inoculated in NVM/CAA+ medium with the corresponding antibiotic, with an optical density of 0.1 and grown at 37 °C with agitation. The optical densities were measured at 600 nm and measurements were taken at regular 24-hour intervals.

Figure 10 shows that the truncated strain of PCNA grows steadily from the start, showing a consistent increase in OD_{600} eventually reaching a peak at around 96 hours. However, after 96 hours**,** the growth curve shows a marked decline, indicating a significant lysis phase. This drop is especially pronounced between 96 and 144 hours.

The control has a delayed growth phase, showing almost no growth until around 48 hours, where it starts an increase, spiking sharply and reaching a higher OD_{600} than the truncated PCNA at around 96 hours.

N. magadii L13 (pRo-5) has a delayed growth initially but experiences a much more aggressive exponential phase, peaking higher than the truncated PCNA before declining rapidly.

Truncated PCNA grows more consistently throughout, with a less dramatic peak and a more stable decline, suggesting it maintains a more controlled growth over time.

3.2.2. Western blot analysis of upstream-mutant methyltransferase

To further explore whether PCNA influences the binding of regulatory elements to ORF94, which encodes the methyltransferase protein, a mutation was introduced in the upstream region of ORF94. This experiment aimed to assess whether the mutation affects the interaction between PCNA and the regulatory elements controlling methyltransferase expression. Western blot analysis was performed to compare methyltransferase protein levels across different PCNA variants. Whole-cell extracts were prepared every 24 hours over seven days from cultures grown in NVM+ medium.

In addition, extracts from *N. magadii* L11 (positive control) and *N. magadii* L13 (negative control) were used to provide a reference for natural methyltransferase production in the presence and absence of ϕCh1. A polyclonal rabbit antibody raised against the methyltransferase protein was used for detection.

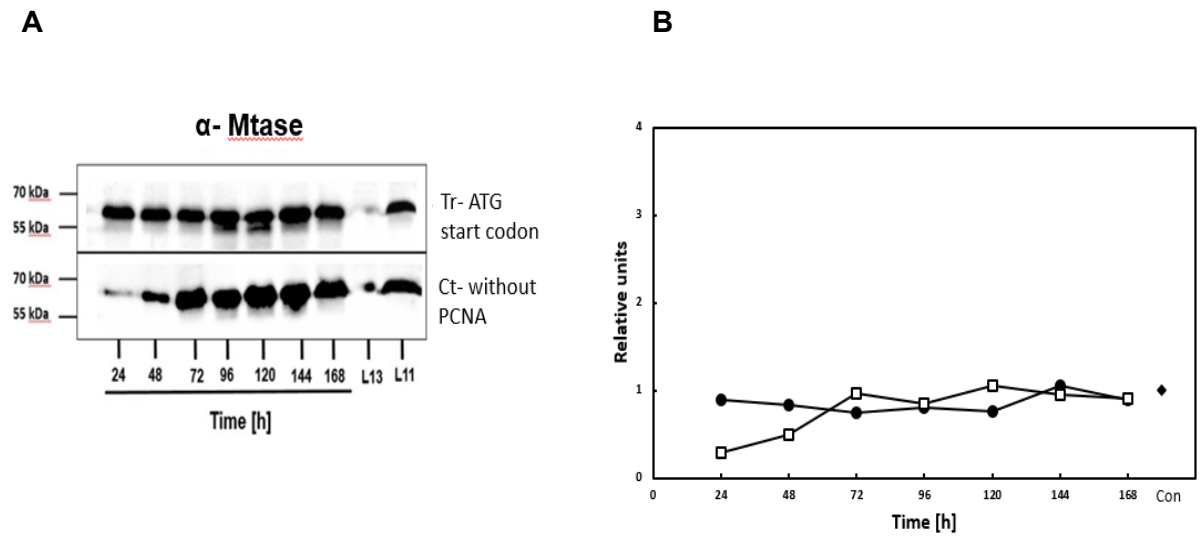

Figure 11. ***A:*** Western blot analysis of *N. magadii* L13 PCNA constructs including truncated version (pRo-5-PCNA-Tr) and the control (pRo-5) with antibody against Mtase. Marker: PageRuler™ Plus Prestained Protein Ladder, 10 to 250 kDa; lane 1-7 (left to right): samples from day 1-7; *N. magadii* L13 negative control; N. magadii L11 positive control. Protein sizes are indicated on the left. **B:** Protein levels of the of *N. magadii* L13 PCNA strains including truncated version (pRo-5-34up-PCNA_Tr) (●), and the control (pRo-5) (❒) as measured by Western blot and analyzed. In addition, L11 cell extract was used a positive control (◆) and set as 1. Densitometry analyses were done using Image lab tool from BioRad.

The Western blot shows that the truncated PCNA variant displays relatively consistent levels, from as early as 24 hours, with a gradual increase in intensity over time indicating that the truncated PCNA supports continuous and steady expression of the methyltransferase (Figure 11). In contrast in the control, methyltransferase expression begins after the 48-hour, however, a significant increase in band intensity is observed after 48 hours. The bands continue to intensify over time, reaching their peak expression between 120 and 144 hours. However, the reduced expression in the truncated variant of PCNA might imply that the truncated form of PCNA struggles to regulate methyltransferase expression, potentially due to altered interactions with the mutated upstream region of ORF94**.**

3.3. Effect of PCNA on tail-fibre gp34 protein expression in *N. magadii*

Since PCNA (Proliferating Cell Nuclear Antigen) is known to interact with various proteins involved in DNA replication, repair, and overall cellular processes through protein-protein interactions, it is possible that PCNA may also influence the expression or activity of other proteins, such as the tail fibre protein that is encoded by ORF34.

To investigate the role of PCNA in tail fibre protein production, a transformation assay was designed. A pRo-5 plasmid containing one of three variants of PCNA ϕCh1 including the mutant variant (pRo-5-PCNA-GTG-ATG) truncated variant (pRo-5-PCNA-Tr), wild-type variant (pRo-5-PCNA-GTG) under the control of the ORF34 promoter was transformed into *N. magadii* L13 cells using a PEG-600 mediated transformation assay.

A clone for the mutant variant of PCNA where GTG is replaced by ATG, was obtained from a colleague who used a Gibson assembly method to generate the construct, in contrast to the other clones that were created with conventional cloning techniques. Despite the different approaches, the mutant PCNA clone provided by the colleague was used for both growth curve analysis and Western blot studies. This allowed for a comparison between the clones, regardless of the cloning method used, ensuring consistency in evaluating the effects of the mutant PCNA on growth and protein expression.

Positive colonies, which successfully integrated the plasmid, were identified using colony PCR (data not shown). Additionally, empty plasmid controls were included in the experiment to serve as a baseline and to ensure any observed changes in tail fibre protein production could be attributed to the presence and function of PCNA variants, rather than nonspecific effects of the plasmid.

By conducting this transformation assay and further Western blot analysis, it became possible to assess whether PCNA directly or indirectly regulates the production of the tail fibre protein encoded by ORF34. This approach not only allows for a comparison of the effects of different PCNA variants but also provides insight into the potential functional or regulatory role that PCNA might have in enhancing or suppressing tail fibre protein synthesis.

3.3.1. Growth kinetics analysis of N. magadii strains expressing the ORF34

To monitor growth dynamics, clones from each strain were selected and tracked over the 7 days (168 hours) course. Optical density at 600 nm (OD_{600}) was measured every 24 hours to generate growth curves and track the growth dynamics of each PCNA variant.

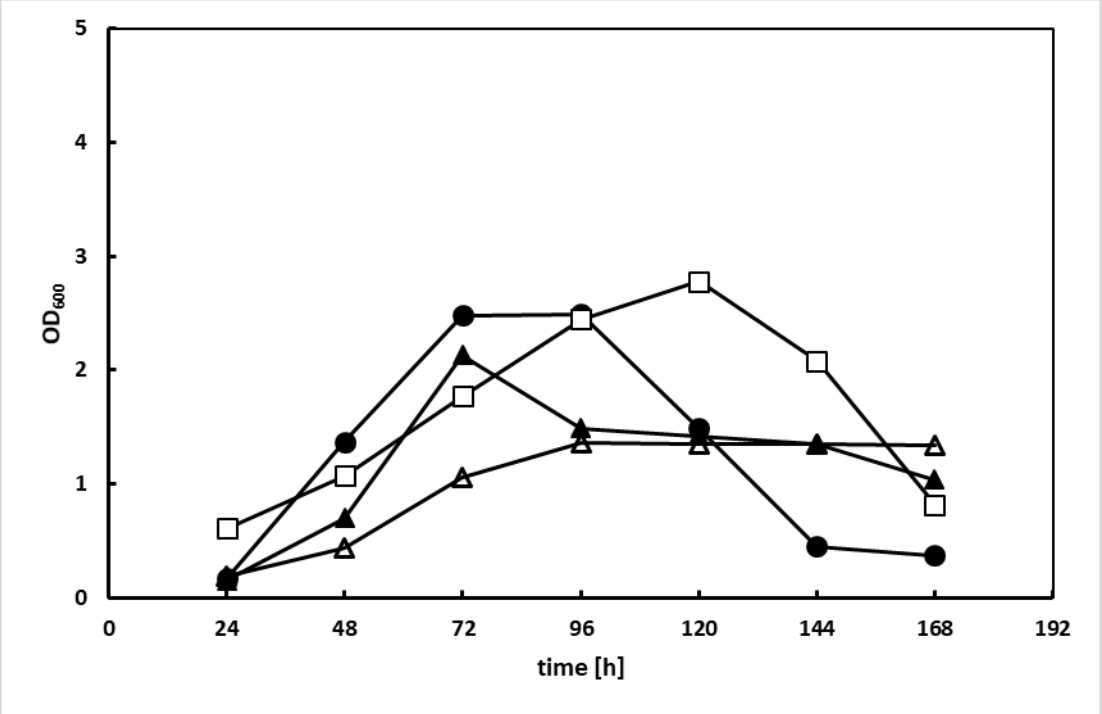

Figure 12. Growth curves of *N. magadii* L13 PCNA constructs including the mutant version (*pRo-5-PCNA-GTG-ATG_ORF34$_{52}$*) (△), truncated version (pRo-5-PCNA-Tr) (●), wild-type version (pRo-5-PCNA-GTG) (▲) and the control (pRo-5) (❒) over the course of 7 days (168 hours). Strains were inoculated in NVM/CAA+ medium with the corresponding antibiotic, with an optical density of 0. 1 and grown at 37 °C with agitation. The optical densities were measured at 600 nm and measurements were taken at regular 24-hour intervals.

As shown in Figure 12, the truncated PCNA variant shows a pattern of initial rapid growth, with the fastest increase observed between 48 and 72 hours**.** However, after 96 hours**,** the growth curve shows a marked decrease of the optical density. This drop is especially pronounced between 96 and 144 hours, suggesting that while the truncated PCNA variant facilitates early and accelerated cell growth, it also leads to an early onset of lysis.

In contrast, the mutant PCNA variant demonstrates a slower initial growth compared to the other constructs. Its peak occurs later, around 96 hours**,** however, it doesn't reach the same peak OD_{600} values as the truncated, wild-type or control strains at this point, indicating a potentially slower growth rate and delayed response. Importantly, the mutant variant does not undergo significant lysis after reaching its peak suggesting that the mutation may be affecting cell stability and lysis regulation**.**

The wild-type PCNA construct shows moderate growth throughout the experiment. Its growth steadily increases, peaking at 72 hours but unlike the truncated variant, the wild-type displays an earlier decline after 72 hours.

The control strain, in the absence of any PCNA variant, exhibits the most rapid and sustained growth throughout the entire course of the experiment. It reaches its peak later than the other constructs, at 120 hours, and although a slight decline in growth is observed after this point, the control strain maintains a relatively high OD_{600} until 168 hours. This indicates slower lysis and overall stronger growth dynamics when compared to the other variants.

3.3.2. Western blot analysis of gp34 production

To further investigate whether PCNA has a direct or indirect effect on gp34 production, Western blot analysis was performed. By comparing gp34 protein levels across different PCNA variants, the results provide insight into PCNA's role in regulating gp34 expression. Whole cell extracts were prepared every 24 hours for seven days from cultures grown in NVM+ medium for analysis. Additionally, extracts from *N. magadii* L11 and *N. magadii* L13 were used as positive and negative controls, respectively. A polyclonal rabbit antibody was raised against the gp34 protein.

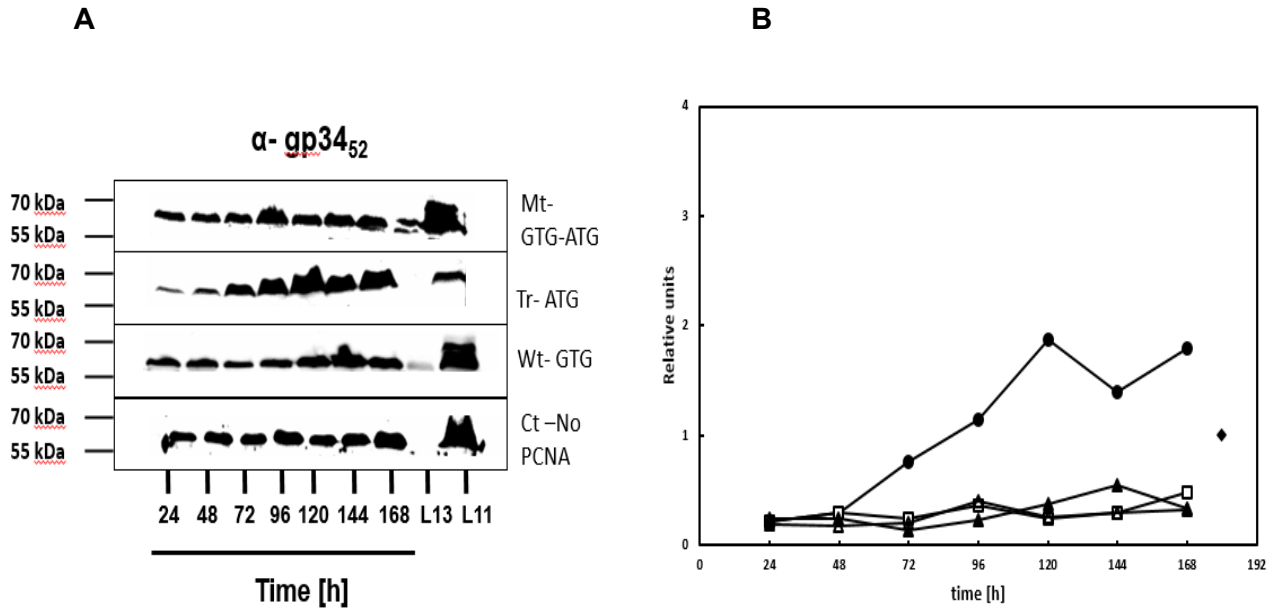

Figure 13. **A:** Western blot analysis of *N. magadii* L13 PCNA constructs including the mutant version (pRo-5-PCNA-GTG-ATG_ORF34$_{52)}$, truncated version (pRo-5-PCNA-Tr), wild-type version (pRo-5-PCNA-GTG) and the control (pRo-5) with antibody against gp34 for time course Marker: PageRuler™ Plus Prestained Protein Ladder, 10 to 250 kDa; lane 1-7 (left to right): sample from day 1-7; *N. magadii* L13 negative control; *N. magadii* L11 positive control. Protein sizes are indicated on the left. **B:** Protein levels of the of *N. magadii* L13 PCNA strains including the mutant version (pRo-5-34up-PCNA_Mt) (△), truncated version (pRo-5-34up-PCNA_Tr) (●), wild-type version (pRo-5-34up-PCNA_WT) (▲) and the control (pRo-5) (❒) as measured by Western blot and analyzed. In addition, L11 cell extract was used a positive control (◆) and set as 1. Densitometry analyses were done using Image lab tool from BioRad.

The Western blot analysis reveals that the mutant PCNA variant displays a gradual increase in band intensity over time, with gp34 expression becoming evident at around 72 hours and reaching its peak at 168 hours. This indicates that the mutant variant has a delayed yet substantial influence on gp34 production.

In the truncated PCNA variant, gp34 expression begins around the 48-hour mark, with an increasing intensity over time. Although the expression pattern is similar to the mutant variant, it appears that the truncated PCNA induces a slightly later response (Figure 13).

In the case of the wild-type PCNA, gp34 expression is constant starting as early as 24 hours. The bands show a gradual increase in intensity throughout the time course, indicating that wild-type PCNA supports continuous and steady gp34 production. This suggests that the natural form of PCNA plays a crucial role in maintaining stable and efficient gp34 expression under these conditions.

When observing the control, we see the gp34 expression is consistent and starts to increase at 144 hours, with the most intense band at 168 hours. This may indicate a baseline level of gp34 production independent of PCNA.

Direct or Indirect Effect? The three PCNA variants influence gp34 expression differently. The mutant PCNA has a stronger and delayed induction of gp34, while the truncated PCNA shows moderate expression. Wild-type PCNA supports consistent, steady gp34 production. The control strain exhibits minimal and delayed gp34 production, suggesting that PCNA plays a direct role in promoting or stabilizing gp34 expression over time. The varying levels of expression across PCNA variants hint at a direct functional impact of PCNA on gp34 production.

4. Conclusion

The focus of this study was to investigate whether PCNA has a direct or indirect role on the expression of methyltransferase and gp34 genes, encoded by ϕCh1, in *Natrialba magadii* L13 strain, a cured strain lacking the ϕCh1 virus.

Proliferating Cell Nuclear Antigen (PCNA) is a scaffold protein primarily involved in DNA replication, interacting with numerous partners. Interestingly, the ϕCh1 virus encodes its own PCNA protein, which is unusual for a virus. *Natrialba magadii*, the only known host of ϕCh1, also produces a similar PCNA, with a key difference in the start codon: the viral PCNA uses an alternative GUG start codon upstream of the typical AUG, leading to a larger protein (Manning *et al.*, 2022b).

In previous research the viral PCNA gene was deleted by homologous recombination which led to a significant decrease in virus titer, reduced viral protein production and diminished lysis. Complementation and overexpression experiments in the L11 wild type strain of *N. magadii* with wild-type and mutant ORF59 variants showed that altering the GTG start codon to ATG affected the virus life cycle, particularly in the production of progeny virus particles. However, the specific influence of PCNA on key viral and host protein expression, particularly methyltransferase and tail-fiber protein gp34, remains unexplored in a virus-cured strain.

In order to determine the effect of PCNA on the expression of methyltransferase and gp34 proteins in *Natrialba magadii* strain L13, three PCNA variants were investigated: (1) the wild-type viral PCNA starting with the GTG codon, (2) a variant with the GTG codon changed to ATG and (3) a truncated version starting with ATG, which is the same size as the host-encoded PCNA. The effect of these PCNA variants was analysed in two systems: in cis**,**

in which PCNA and the target gene (gp34) were located on the same plasmid, and in trans**,** in which PCNA and ORF94 (methyltransferase) were expressed from separate plasmids.

Two shuttle vectors, pNB102 and pRo-5, were used for the co-transformation assay. The pNB102 plasmid, containing ORF94 with its own promoter sequence, and pRo-5 plasmid, containing one of three variants of PCNA ϕCh1 under the control of the ORF34 promoter, were cloned into *N. magadii* L13.

In addition to the wild-type ORF94 construct, a second variant named pNB102-ORF94-M-M1_2, was introduced. This construct contains a mutated upstream region of ORF94 (ORF94-M-M1_2), specifically designed to investigate whether alterations in the upstream regulatory region affect the binding and subsequent expression of the methyltransferase.

Growth curves and protein expression analyses, particularly via Western blot, were performed to assess the impact of each PCNA variant on both genes.

The truncated version of $PCNA_{\phi Ch1}$ demonstrated a distinct regulatory profile, particularly influencing the methyltransferase gene (ORF94) and the tail fibre gene (ORF34). Notably, the truncated variant led to an increase and earlier expression of the methyltransferase gene in comparison to the wild-type.

With mutations in the upstream region (putative promoter) of the methyltransferase gene (ORF94), the truncated version of $PCNA_{\phi Ch1}$ shows almost constitutive expression of the Mtase gene, suggesting a loss of proper regulatory modulation.

The truncated version of PCNA $_{\phi Ch1}$ specifically leads to the overexpression of the tail fibre gene ORF34, a regulatory effect that is uniquely associated with this variant and is not observed with any of the other PCNA versions analyzed in this study.

The truncated PCNA $_{\phi Ch1}$ was also found to resemble the host-encoded PCNA in its ability to increase the copy number of the target plasmid.

Additionally, the N-terminal extension present in the wild-type PCNA $_{\phi Ch1}$ appears to play a significant role in maintaining proper gene regulation. This extension, which is absent in the truncated variant, has been implicated in increasing the number of progeny viruses, underscoring its importance for viral replication and gene regulation. Together, these findings provide valuable insights into how specific structural features of PCNA, including its truncation, can modulate the expression of key viral genes.

References

Ackermann, H.-W., Prangishvili, D., 2012. Prokaryote viruses studied by electron microscopy. Arch. Virol. 157, 1843–1849. https://doi.org/10.1007/s00705-012-1383-y

Albers, S.-V., Meyer, B.H., 2011. The archaeal cell envelope. Nat. Rev. Microbiol. 9, 414–426. https://doi.org/10.1038/nrmicro2576

Andrei, A.-Ş., Banciu, H.L., Oren, A., 2012. Living with salt: metabolic and phylogenetic diversity of archaea inhabiting saline ecosystems. FEMS Microbiol. Lett. 330, 1–9. https://doi.org/10.1111/j.1574-6968.2012.02526.x

Arnold, H.P., Zillig, W., Ziese, U., Holz, I., Crosby, M., Utterback, T., Weidmann, J.F., Kristjanson, J.K., Klenk, H.P., Nelson, K.E., Fraser, C.M., 2000. A Novel Lipothrixvirus, SIFV, of the Extremely Thermophilic Crenarchaeon Sulfolobus. Virology 267, 252–266. https://doi.org/10.1006/viro.1999.0105

Arrías, P.N., Monzon, A.M., Clementel, D., Mozaffari, S., Piovesan, D., Kajava, A.V., Tosatto, S.C.E., 2023. The repetitive structure of DNA clamps: An overlooked protein tandem repeat. J. Struct. Biol. 215, 108001. https://doi.org/10.1016/j.jsb.2023.108001

Babski, J., Haas, K.A., Näther-Schindler, D., Pfeiffer, F., Förstner, K.U., Hammelmann, M., Hilker, R., Becker, A., Sharma, C.M., Marchfelder, A., Soppa, J., 2016. Genome-wide identification of transcriptional start sites in the haloarchaeon Haloferax volcanii based on differential RNA-Seq (dRNA-Seq). BMC Genomics 17, 629. https://doi.org/10.1186/s12864-016-2920-y

Baranyi, U., Klein, R., Lubitz, W., Kru, D.H., Witte, A., 2000. The archaeal halophilic virus-encoded Dam-like methyltransferase M.fCh1-I methylates adenine residues and complements dam mutants in the low salt environment of Escherichia coli. Mol. Microbiol.

Bernander, R., 2000. Chromosome replication, nucleoid segregation and cell division in Archaea. Trends Microbiol. 8, 278–283. https://doi.org/10.1016/S0966-842X(00)01760-1

Bitan-Banin, G., Ortenberg, R., Mevarech, M., 2003. Development of a Gene Knockout System for the Halophilic Archaeon *Haloferax volcanii* by Use of the *pyrE* Gene. J. Bacteriol. 185, 772–778. https://doi.org/10.1128/JB.185.3.772-778.2003

Breuert, S., Allers, T., Spohn, G., Soppa, J., 2006. Regulated Polyploidy in Halophilic Archaea. PLoS ONE 1, e92. https://doi.org/10.1371/journal.pone.0000092

Brochier-Armanet, C., Boussau, B., Gribaldo, S., Forterre, P., 2008. Mesophilic crenarchaeota: proposal for a third archaeal phylum, the Thaumarchaeota. Nat. Rev. Microbiol. 6, 245–252. https://doi.org/10.1038/nrmicro1852

Charlebois, R.L., Lam, W.L., Cline, S.W., Doolittle, W.F., 1987. Characterization of pHV2 from Halobacterium volcanii and its use in demonstrating transformation of an archaebacterium. Proc. Natl. Acad. Sci. 84, 8530–8534. https://doi.org/10.1073/pnas.84.23.8530

Christian, J.H.B., Waltho, J.A., 1962. Solute concentrations within cells of halophilic and non-halophilic bacteria. Biochim. Biophys. Acta 65, 506–508. https://doi.org/10.1016/0006-3002(62)90453-5

Cline, S.W., Doolittle, W.F., 1987. Efficient transfection of the archaebacterium Halobacterium halobium. J. Bacteriol. 169, 1341–1344. https://doi.org/10.1128/jb.169.3.1341-1344.1987

De La Haba, R.R., Sánchez-Porro, C., Marquez, M.C., Ventosa, A., 2011. Taxonomy of Halophiles, in: Horikoshi, K. (Ed.), Extremophiles Handbook. Springer Japan, Tokyo, pp. 255–308. https://doi.org/10.1007/978-4-431-53898-1_13

Dellas, N., Snyder, J.C., Bolduc, B., Young, M.J., 2014. Archaeal Viruses: Diversity, Replication, and Structure. Annu. Rev. Virol. 1, 399–426. https://doi.org/10.1146/annurev-virology-031413-085357

DeLong, E.F., 1992. Archaea in coastal marine environments. Proc. Natl. Acad. Sci. 89, 5685–5689. https://doi.org/10.1073/pnas.89.12.5685

Dyall-Smith, M., Tang, S.-L., Bath, C., 2003. Haloarchaeal viruses: how diverse are they? Res. Microbiol. 154, 309–313. https://doi.org/10.1016/S0923-2508(03)00076-7

Edwards, M.A., 2018. Stability of the ΦCh1 ORF44 deletion mutant and characterization of the function of gp44.

Fendrihan, S., Legat, A., Pfaffenhuemer, M., Gruber, C., Weidler, G., Gerbl, F., Stan-Lotter, H., 2006. Extremely halophilic archaea and the issue of long-term microbial survival. Rev. Environ. Sci. Biotechnol. 5, 203–218. https://doi.org/10.1007/s11157-006-0007-y

Häring, M., Rachel, R., Peng, X., Garrett, R.A., Prangishvili, D., 2005. Viral Diversity in Hot Springs of Pozzuoli, Italy, and Characterization of a Unique Archaeal Virus, *Acidianus* Bottle-Shaped Virus, from a New Family, the *Ampullaviridae*. J. Virol. 79, 9904–9911. https://doi.org/10.1128/JVI.79.15.9904-9911.2005

Hartman, R., Munson-McGee, J., Young, M.J., Lawrence, C.M., 2019. Survey of high-resolution archaeal virus structures. Curr. Opin. Virol. 36, 74–83. https://doi.org/10.1016/j.coviro.2019.05.008

Iranzo, J., Krupovic, M., Koonin, E.V., 2016. The Double-Stranded DNA Virosphere as a Modular Hierarchical Network of Gene Sharing. mBio 7, e00978-16. https://doi.org/10.1128/mBio.00978-16

Iro, M., Klein, R., Gálos, B., Baranyi, U., Rössler, N., Witte, A., 2007. The lysogenic region of virus ϕCh1: identification of a repressor-operator system and determination of its activity in halophilic Archaea. Extremophiles 11, 383–396. https://doi.org/10.1007/s00792-006-0040-3

Janekovic, D., Wunderl, S., Holz, I., Zillig, W., Gierl, A., Neumann, H., 1983. TTV1, TTV2 and TTV3, a family of viruses of the extremely thermophilic, anaerobic, sulfur reducing archaebacterium Thermoproteus tenax. Mol. Gen. Genet. MGG 192, 39–45. https://doi.org/10.1007/BF00327644

Kamekura, M., Dyall-Smith, M.L., Upasani, V., Ventosa, A., Kates, M., 1997. Diversity of Alkaliphilic Halobacteria: Proposals for Transfer of Natronobacterium vacuolatum, Natronobacterium magadii, and Natronobacterium pharaonis to Halorubrum, Natrialba, and Natronomonas gen. nov., Respectively, as Halorubrum vacuolatum comb. nov., Natrialba magadii comb. nov., and Natronomonas pharaonis comb. nov., Respectively. Int. J. Syst. Bacteriol. 47, 853–857. https://doi.org/10.1099/00207713-47-3-853

Kelman, Z., 1997. PCNA: structure, functions and interactions. Oncogene 14, 629–640. https://doi.org/10.1038/sj.onc.1200886

Klein, R., Baranyi, U., Rössler, N., Greineder, B., Scholz, H., Witte, A., 2002. *Natrialba magadii* virus **ϕ** Ch1: first complete nucleotide sequence and functional organization of a virus infecting a haloalkaliphilic archaeon. Mol. Microbiol. 45, 851–863. https://doi.org/10.1046/j.1365-2958.2002.03064.x

Klein, R., Rössler, N., Iro, M., Scholz, H., Witte, A., 2012. Haloarchaeal myovirus ϕCh1 harbours a phase variation system for the production of protein variants with distinct cell surface adhesion specificities. Mol. Microbiol. 83, 137–150. https://doi.org/10.1111/j.1365-2958.2011.07921.x

Krupovic, M., Cvirkaite-Krupovic, V., Iranzo, J., Prangishvili, D., Koonin, E.V., 2018. Viruses of archaea: Structural, functional, environmental and evolutionary genomics. Virus Res. 244, 181–193. https://doi.org/10.1016/j.virusres.2017.11.025

Krupovic, M., Quemin, E.R.J., Bamford, D.H., Forterre, P., Prangishvili, D., 2014. Unification of the Globally Distributed Spindle-Shaped Viruses of the Archaea. J. Virol. 88, 2354–2358. https://doi.org/10.1128/JVI.02941-13

Lai, M.C., Gunsalus, R.P., 1992. Glycine betaine and potassium ion are the major compatible solutes in the extremely halophilic methanogen Methanohalophilus strain Z7302. J. Bacteriol. 174, 7474–7477. https://doi.org/10.1128/jb.174.22.7474-7477.1992

Lai, M.C., Sowers, K.R., Robertson, D.E., Roberts, M.F., Gunsalus, R.P., 1991. Distribution of compatible solutes in the halophilic methanogenic archaebacteria. J. Bacteriol. 173, 5352–5358. https://doi.org/10.1128/jb.173.17.5352-5358.1991

Lam, W.L., Doolittle, W.F., 1992. Mevinolin-resistant mutations identify a promoter and the gene for a eukaryote-like 3-hydroxy-3-methylglutaryl-coenzyme A reductase in the archaebacterium Haloferax volcanii. J. Biol. Chem. 267, 5829–5834. https://doi.org/10.1016/S0021-9258(18)42628-2

Lanyi, J.K., n.. Salt-Dependent Properties of Proteins from Extremely Halophilic Bacteria. BACTERIOL REV.

Luk, A., Williams, T., Erdmann, S., Papke, R., Cavicchioli, R., 2014. Viruses of Haloarchaea. Life 4, 681–715. https://doi.org/10.3390/life4040681

Ma, Y., Galinski, E.A., Grant, W.D., Oren, A., Ventosa, A., 2010. Halophiles 2010: Life in Saline Environments. Appl. Environ. Microbiol. 76, 6971–6981. https://doi.org/10.1128/AEM.01868-10

Maga, G., Hübscher, U., 2003. Proliferating cell nuclear antigen (PCNA): a dancer with many partners. J. Cell Sci. 116, 3051–3060. https://doi.org/10.1242/jcs.00653

Manning, R.J., Tschurtschenthaler, M., Sabitzer, S., Witte, A., 2022a. Manipulation of viral protein production using the PCNA of halovirus ϕCh1 via alternative start codon usage. Curr. Res. Biotechnol. 4, 428–438. https://doi.org/10.1016/j.crbiot.2022.09.006

Manning, R.J., Tschurtschenthaler, M., Sabitzer, S., Witte, A., 2022b. Manipulation of viral protein production using the PCNA of halovirus ϕCh1 via alternative start codon usage. Curr. Res. Biotechnol. 4, 428–438. https://doi.org/10.1016/j.crbiot.2022.09.006

Martin, A., Yeats, S., Janekovic, D., Reiter, W.-D., Aicher, W., Zillig, W., 1984. SAV 1, a temperate u.v.-inducible DNA virus-like particle from the archaebacterium *Sulfolobus acidocaldarius* isolate B12. EMBO J. 3, 2165–2168. https://doi.org/10.1002/j.1460-2075.1984.tb02107.x

Mayrhofer-Iro, M., Ladurner, A., Meissner, C., Derntl, C., Reiter, M., Haider, F., Dimmel, K., Rössler, N., Klein, R., Baranyi, U., Scholz, H., Witte, A., 2013. Utilization of Virus φCh1 Elements To Establish a Shuttle Vector System for Halo(alkali)philic Archaea via Transformation of Natrialba magadii. Appl. Environ. Microbiol. 79, 2741–2748. https://doi.org/10.1128/AEM.03287-12

Mengele, R., Sumper, M., 1992. Drastic differences in glycosylation of related S-layer glycoproteins from moderate and extreme halophiles. J. Biol. Chem. 267, 8182–8185. https://doi.org/10.1016/S0021-9258(18)42424-6

Mescher, M.F., Strominger, J.L., 1976. Purification and characterization of a prokaryotic glycoprotein from the cell envelope of Halobacterium salinarium. J. Biol. Chem. 251, 2005–2014. https://doi.org/10.1016/S0021-9258(17)33647-5

Moldovan, G.-L., Pfander, B., Jentsch, S., 2007. PCNA, the Maestro of the Replication Fork. Cell 129, 665–679. https://doi.org/10.1016/j.cell.2007.05.003

Ng, W.L., DasSarma, S., 1993. Minimal replication origin of the 200-kilobase Halobacterium plasmid pNRC100. J. Bacteriol. 175, 4584–4596. https://doi.org/10.1128/jb.175.15.4584-4596.1993

Olsen, G.J., Woese, C.R. Archaeal Genomics: An Overview Minireview.

Oren, A., 2014. Taxonomy of halophilic Archaea: current status and future challenges. Extremophiles 18, 825–834. https://doi.org/10.1007/s00792-014-0654-9

Oren, A., 1999. Bioenergetic Aspects of Halophilism. Microbiol. Mol. Biol. Rev. 63, 334–348. https://doi.org/10.1128/MMBR.63.2.334-348.1999

Oren, A. Diversity of halophilic microorganisms: Environments, phylogeny, physiology, and applications.

Pan, M., Santangelo, T.J., Čuboňová, Ľ., Li, Z., Metangmo, H., Ladner, J., Hurwitz, J., Reeve, J.N., Kelman, Z., 2013. Thermococcus kodakarensis has two functional PCNA homologs but only one is required for viability. Extremophiles 17, 453–461. https://doi.org/10.1007/s00792-013-0526-8

Pietilä, M.K., Demina, T.A., Atanasova, N.S., Oksanen, H.M., Bamford, D.H., 2014. Archaeal viruses and bacteriophages: comparisons and contrasts. Trends Microbiol. 22, 334–344. https://doi.org/10.1016/j.tim.2014.02.007

Pietilä, M.K., Laurinmäki, P., Russell, D.A., Ko, C.-C., Jacobs-Sera, D., Butcher, S.J., Bamford, D.H., Hendrix, R.W., 2013. Insights into Head-Tailed Viruses Infecting Extremely Halophilic Archaea. J. Virol. 87, 3248–3260. https://doi.org/10.1128/JVI.03397-12

Pikuta, E.V., Hoover, R.B., Tang, J., 2007. Microbial Extremophiles at the Limits of Life. Crit. Rev. Microbiol. 33, 183–209. https://doi.org/10.1080/10408410701451948

Porter, K., Russ, B.E., Dyall-Smith, M.L., 2007. Virus–host interactions in salt lakes. Curr. Opin. Microbiol. 10, 418–424. https://doi.org/10.1016/j.mib.2007.05.017

Prangishvili, D., 2013. The Wonderful World of Archaeal Viruses. Annu. Rev. Microbiol. 67, 565–585. https://doi.org/10.1146/annurev-micro-092412-155633

R. Klein, U. Baranyi, N. Rössler, B. Greineder, H. Scholz, and A. Witte

Rodrigues-Oliveira, T., Belmok, A., Vasconcellos, D., Schuster, B., Kyaw, C.M., 2017. Archaeal S-Layers: Overview and Current State of the Art. Front. Microbiol. 8, 2597. https://doi.org/10.3389/fmicb.2017.02597

Roine, E., Oksanen, H.M., 2011. Viruses from the Hypersaline Environment, in: Ventosa, A., Oren, A., Ma, Y. (Eds.), Halophiles and Hypersaline Environments. Springer Berlin Heidelberg, Berlin, Heidelberg, pp. 153–172. https://doi.org/10.1007/978-3-642-20198-1_8

Schnabel, H., Zillig, W., Pfäffle, M., Schnabel, R., Michel, H., Delius, H., 1982. *Halobacterium halobium* phage øH. EMBO J. 1, 87–92. https://doi.org/10.1002/j.1460-2075.1982.tb01129.x

Senčilo, A., Roine, E., 2014. A Glimpse of the genomic diversity of haloarchaeal tailed viruses. Front. Microbiol. 5. https://doi.org/10.3389/fmicb.2014.00084

Sleytr & Beveridge, 1999

Soliman, G.S.H., Trüper, H.G., 1982. Halobacterium pharaonis sp. nov., a New, Extremely Haloalkaliphilic Archaebacterium with Low Magnesium Requirement. Zentralblatt Für Bakteriol. Mikrobiol. Hyg. Abt Orig. C Allg. Angew. Ökol. Mikrobiol. 3, 318–329. https://doi.org/10.1016/S0721-9571(82)80045-8

Sorokin, D.Y., Elcheninov, A.G., Toshchakov, S.V., Bale, N.J., Sinninghe Damsté, J.S., Khijniak, T.V., Kublanov, I.V., 2019. Natrarchaeobius chitinivorans gen. nov., sp. nov., and Natrarchaeobius halalkaliphilus sp. nov., alkaliphilic, chitin-utilizing haloarchaea from hypersaline alkaline lakes. Syst. Appl. Microbiol. 42, 309–318. https://doi.org/10.1016/j.syapm.2019.01.001

Sorokin, D.Y., Khijniak, T.V., Kostrikina, N.A., Elcheninov, A.G., Toshchakov, S.V., Bale, N.J., Damsté, J.S.S., Kublanov, I.V., 2018. Natronobiforma cellulositropha gen. nov., sp. nov., a novel haloalkaliphilic member of the family Natrialbaceae (class Halobacteria) from hypersaline alkaline lakes. Syst. Appl. Microbiol. 41, 355–362. https://doi.org/10.1016/j.syapm.2018.04.002

Stoimenov, I., Helleday, T., 2009. PCNA on the crossroad of cancer. Biochem. Soc. Trans. 37, 605–613. https://doi.org/10.1042/BST0370605

Tang, S., Nuttall, S., Ngui, K., Fisher, C., Lopez, P., Dyall-Smith, M., 2002. HF2: a double-stranded DNA tailed haloarchaeal virus with a mosaic genome. Mol. Microbiol. 44, 283–296. https://doi.org/10.1046/j.1365-2958.2002.02890.x

Tenchov, B., Vescio, E.M., Sprott, G.D., Zeidel, M.L., Mathai, J.C., 2006. Salt Tolerance of Archaeal Extremely Halophilic Lipid Membranes. J. Biol. Chem. 281, 10016–10023. https://doi.org/10.1074/jbc.M600369200

Tindall, B.J., Ross, H.N.M., Grant, W.D., 1984. Natronobacterium gen. nov. and Natronococcus gen. nov., Two New Genera of Haloalkaliphilic Archaebacteria. Syst. Appl. Microbiol. 5, 41–57. https://doi.org/10.1016/S0723-2020(84)80050-8

Torsvik and Dundas, 1974

Torsvik, T., Dundas, I.D., 1980. Persisting Phage Infection in Halobacterium salinarium str. 1. J. Gen. Virol. 47, 29–36. https://doi.org/10.1099/0022-1317-47-1-29

Valentine, D.L., 2007. Adaptations to energy stress dictate the ecology and evolution of the Archaea. Nat. Rev. Microbiol. 5, 316–323. https://doi.org/10.1038/nrmicro1619

Van De Vossenberg, J. L. C. M. *et al.* (1999)

Wais *et al.*, 1975
Williams, T.A., Cox, C.J., Foster, P.G., Szöllősi, G.J., Embley, T.M., 2019. Phylogenomics provides robust support for a two-domains tree of life. Nat. Ecol. Evol. 4, 138–147. https://doi.org/10.1038/s41559-019-1040-x
Willmer, P.G., 2000. Extremophiles in the raw. Nature 408, 771–771. https://doi.org/10.1038/35048631
Witte, A., Baranyi, U., Klein, R., Sulzner, M., Luo, C., Wanner, G., 1997. Characterization of Natronobacteriummagadii phage FCh1, a unique archaeal phage containing DNA and RNA.
Woese, C.R. 1990 Towards a natural system of organisms: Proposal for the domains Archaea, Bacteria, and Eucarya.
Woese, C.R., Fox, G.E., 1977. Phylogenetic structure of the prokaryotic domain: The primary kingdoms. Proc. Natl. Acad. Sci. 74, 5088–5090. https://doi.org/10.1073/pnas.74.11.5088
Xue, Y., Fan, H., Ventosa, A., Grant, W.D., Jones, B.E., Cowan, D.A., Ma, Y., 2005. Halalkalicoccus tibetensis gen. nov., sp. nov., representing a novel genus of haloalkaliphilic archaea. Int. J. Syst. Evol. Microbiol. 55, 2501–2505. https://doi.org/10.1099/ijs.0.63916-0
Zhou, M., Xiang, H., Sun, C., Tan, H., 2004. Construction of a novel shuttle vector based on an RCR-plasmid from a haloalkaliphilic archaeon and transformation into other haloarchaea. Biotechnol. Lett. 26, 1107–1113. https://doi.org/10.1023/B:BILE.0000035493.21986.20